A Study on the Electromechanical Response of Polyvinylidene Fluoride Base Electroactive Polymers

by

Yancen Cai

A thesis submitted to the Graduate Faculty of
Auburn University
in partial fulfillment of the
requirements for the Degree of
Master of Science

Auburn, Alabama
December 15, 2018

Keywords: electroactive polymer, IPMC, polyvinylidene fluoride, cobalt perchlorate, ions accumulation, back relaxation

Approved by

Zhongyang Cheng, Chair, Professor of Materials Engineering
Edward Davis, Professor of Materials Engineering
Pengyu Chen, Professor of Materials Engineering

Abstract

A novel ionic polymer metal composite (IPMC) actuator based on partially fluorinated ionomer composed of polyvinylidene fluoride (PVDF) and perchlorate is successfully developed. The PVDF-base films are prepared by solution casting, followed by electroding with gold (Au). Unlike other commercial Nafion-base IPMCs, the PVDF film doped with 15 wt.% Cobalt perchlorate (Cop) is the first one of electroactive polymers which show large cathode deformation. 3.5V DC is lowest drive voltage and best electromechanical behavior is shown under 4V DC. Over 250° of bending angle and less than 30s of response time are observed. A CCD camera records the deformation history, Tracker software is used to analyze video and bending angle can be calculated by Newton method. In high humidity (43%), PVDF-CoP film shows fast cathode deformation, followed by positive back relaxation when the DC electric field still applied on. While the PVDF-base IPMC doped with 7.5 wt.% lithium perchlorate (Lip) display anode deformation without any back relaxation. It means that the different cations can be tailored to obtain a desired actuation response. The actuation process depends on size difference between cation and anions. It is discovered that back relaxation will disappear when humidity down to 33%. If humidity low enough (23%), samples show maximum bending without back relaxation. We have reason to believe that hydration reaction of cations could largen the diameter of hydrated cations. It leads to decrease the size difference between hydrated cations and anions.

Table of Contents

List of Figures

List of Tables

Chapter 1: Introduction and Research Objectives

1.1 Fundamentals of Electroactive Polymers (EAPs), their Background and Significance

Electroactive polymers(EAPs) are a novel group of smart materials with unique electrical and mechanical properties.[1]EAPs exhibit a significant shape and size change when stimulated by an electric field.[2]Due to outstanding electrostrictive response, EAPs not only can be used as bidirectional material like actuators and sensors, but also can be apply in biomimetic area such as artificial muscles.

Since the discovery of EAPs in the seventh decade of last century, EAPs did not attach enough importance to actuator because of their low capability. [3]However, actuators based on electroactive polymers (EAPs) have attracted a great deal of interest for past decades due to their electrical energy consumption, light weight compatibility, and compliant ability properties, bio to operate in air and aquatic media, insensitivity to magnetic fields and simple fabrication processes.[4].While today's piezoelectric actuators only deform by a fraction of a percent, EAPs can exhibit a strain of up to 380%.[3]They have the potential for application in the field of biologically devices and robots because the manmade actuators are most closely emulate natural muscles. Therefore, EAP materials have earned the named “artificial muscles”. [3]The Dr. Yoseph Bar-Cohen, JPL, NASA, organized an arm-wresting match between robotic hand made by EAPs and human hand in 1999 (**Figure 1**). The contemporary aim at improving EAPs product performance and enable to create better artificial muscles in lower cost

with greater force. [5]At the same time, the toy industries are benefiting from EAPs. The first commercial entertainment EAPs product was a robot fish which developed by Eamex, Japan in 1999. [5]With the research over the past decade, EAPs have become more stable, but these problems are not completely resolved. In recent years, research concerning EAPs materials has expanded more in terms of getting higher efficiency, lower driving voltage, larger actuation strain and shorter response time. [4]

Figure 1: An artistic interpretation of the Grand Challenge for the development of EAP actuated robotics [5]

At present, based on activation mechanism, EAPs can be basically divided into two types: electronic EAPs and ionic EAPs.

1.1.1 Electronic EAPs

Electronic EAPs (*e* -EAP), also named as field-activated EAPs (FEAPs) are used broadly and of great significance in worldwide. It should be noted that FEAPs exhibit excellent performances, such as high flexibility, light weight, high stress impact resistance, and easy processing. Coulomb force drive *e*-EAP to bend, stretch and contract. The deformation of *e*-EAP can be occurred in air

without any liquid electrolyte. However, it needs a very high driving voltage (>100MV/m) which is close to breakdown level. [6]

Silicone is a common material used in the creation of dielectric elastomers (an *e*-EAP). It can achieve electromechanical strains upwards of 2% at ±3 V DC with response times of under 4s and energy densities reaching 7 Wh/kg. [7][8][9].

The mechanisms of EAPs materials can be subdivide by two main parts: Maxwell stress and electrostriction. In theory, Maxwell's stress can be obtained from free charges on two side of dielectric materials when extra DC electric field applied on it. [10]Zhenyi et al. reported that polyurethane which is a nanocrystalline polymer showed 10% of actuated strain due to Maxwell stress. [11]As displayed in **Figure 2**, a dielectric elastomer film, a typically *e*-EAP martial, is coated with thin gold layer as electrode on two sides. Sample would be stretch due to compress between top and bottom surface when high DC voltage applied on it.

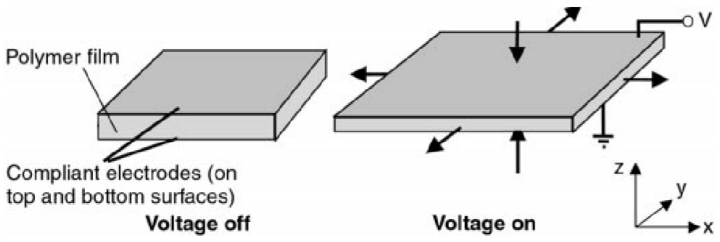

Figure 2：The dielectric elastomers actuate by means of electrostatic forces applied via compliant electrodes on the elastomer film.[12]

For electrostrictive martials, sample size and shape change with dipole density before and after applied DC voltage whether they are crystalline or amorphous. To be specific, if polarization direction is X direction, while the expansion direction is Y direction. [7]However, the electrostriction stain is too

small to be an actuator. *E*-EAP materials show large strain and short response time, but the high driving force limits them application.

1.1.2 Ionic EAPs

Ionic EAP is a very common type in EAPs materials. It consists of two thin metal layers as electrode and polymer solid electrolyte which is doped with mobility ions. [4]Ions can be treated as charged carrier when external electric field applied. So, the barrier of *i*-EAP activation is very low. It means that *i*-EAP actuator can be used in low voltage (<10V). Ions redistribution and accumulation with time is contribute to *i*-EAP actuator bending displacement. *I*-EAP could be divide into main 4 types: Ionic polymer gels, ionic polymers-metal composites, conductive polymers and carbon nanotubes. [4]Different size of ions may lead to different electrostatic pressure in a bending processing. Particularly, ionic polymers-metal composites (IPMC) have received significant research interest over the past decade after discovering by three group of scientists from Japan and United States.

Presented in **Figure 3** is the mechanism of bending process. Classically, ions, doped into polymer film, can be divided into two types: positive (cations) and negative (anions). Among which, cations are free and often combine with water molecules formed hydrated cation while anions usually fix at the end of branch chain. Both cations and anions distribute randomly and uniformly in polymer matrix. When voltage applied on it, only hydrated cation moves to cathode due to coulomb force. With the time going, an increasing number of

hydrated cations accumulate in cathode and then generate pressure which results bending. This process is very similar with natural muscles response.

Compared to *e*-EAP martials, IPMC actuators exhibit large bending strain under low driving voltage. Most IPMC martials excel in some advantages like low-mass and high strain.

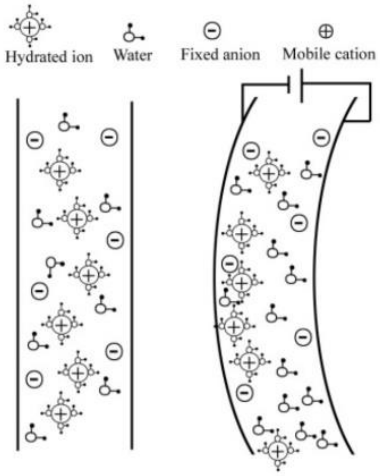

Figure 3: Illustration the cross-section of IPMC actuation mechanism [4]

E-EAPs need high driving voltage to exhibit lager work density, while *i*-EAP can bend in low electric field but the work density also low. The mechanics properties of some smart materials are summarized in **Table 1.** [4]IPMC is a subset of *i*-EAP and has potential as an actuator in large defamation and high efficiency.

Table 1:Comparison of an IPMC with other smart materials

Smart Materials	Strain (%)	Stress (MPa)	Efficiency (%)
Piezoelectric	0.1	35	>75
Magneto strictive	0.2	-	<50
SMA	>4	>300	>3.8
IPMC	>40	>0.3	>30

1.2 Commercial Ionic EAP Materials (Nafion and Flemion)

Nafion (perfluorinated sulfonic acid) is the first commercialized IMPC materials, which was widely used in last years in the field of fuel cells, electrochemical energy storage device, batteries, etc. [13]Nafion is a typically perfluorinated polymers with short branch chain fixed anion. The chemical formula of Nafion is displayed in **Figure 4**.

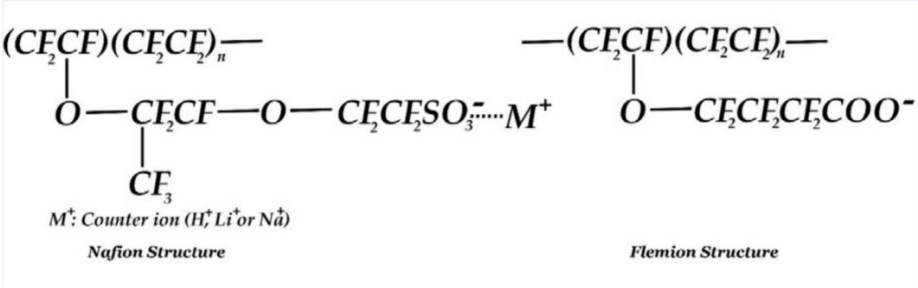

Figure 4: Chemical formulas of Nafion® and Flemion® [1]

In material field, properties are determined by structure, so is IPMC. The polytetrafluoroethylene (PTFE) backbones have effect on their mechanical properties such as stress strength, strain and Yong's modules. The perfluoro branched chain not only can fix anions but also reduce the glass transition temperature (Tg) to make sure polymer is in rubbery state in room temperature. However, the side chain with a sulfonic acid group would damp ions motion. As the result, both ionic conductivity and strain will be limit.

Alkali metal cations such as Li^+, Na^+, K^+, and Rb^+ can be adopted in Nafion bare membrane. Different cations yield different bending angle and speed for the same Nafion film. [4]The process of polymer metallization is that Nafion film is soaked in a salt solution to allow cations to diffuse in. However, it is hard to control the concentrations of cations and the metallic cations are not

homogeneously distributed. Predictably, the concentration of cations near the surface is higher than what is in film center. The surface electroding process is a chemical process. The primary reaction (**Equation. 1.1**) is showed. [14]

$$NaBH_4 + 4[Pt(NH_3)_4]_2^{2+} + 8OH^- \Rightarrow 4Pt + 16NH_3 + NaBO_2 + 6H_2O \quad (1.1)$$

Figure 5 shows the whole process of impregnation-reduction. Major steps include: surface roughening and cleaning, swelling complete, platinum ions immersion and surface electrode reduction.

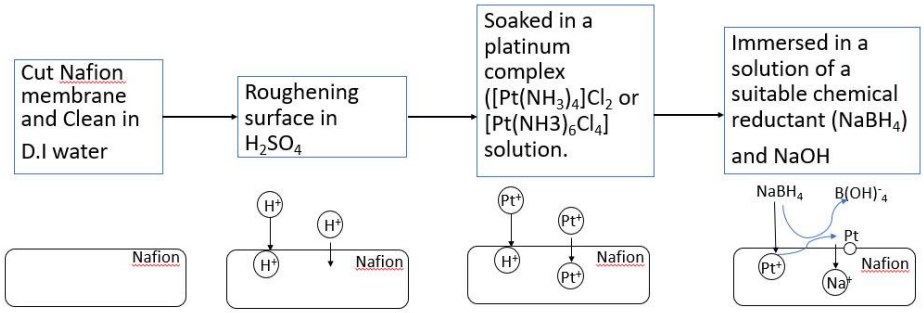

Figure 5: An impregnation-reduction method to prepare Nafion-base IPMC

Flemion, like Nafion, is also a commercialized perfluorinated polymer. **Figure 4** shows the chemical formulas of Flemion. Dry Nafion-based or Flemion-based IMPC cannot bending when electric filed applied. So IMPC sample need solvated or hydrated. To make sure sample fully hydrated, actuation test in water bath because hydrated IPMC sample dries vert fast in open air. [15]So, it is a limit for research and application in our daily life.

1.3 Current Actuation Monitoring Methods

The bending of IPMCs is computed in a cantilever configuration. It means that one end of sample is fixed while the other end is set free. The blocking force with actuation frequency can be measured, as shown in **Figure 6(a)**. The stiffness

of actuator also can be measured (**Figure 6(b)**). Typical time or frequency dependent test is shown in **Figure 6(c)**. However, A large deformation of IPMC is hard to detected by laser sensor. In this paper, a new testing system for tip bending tracking, based on Newton iteration method, will be introduced in detail.

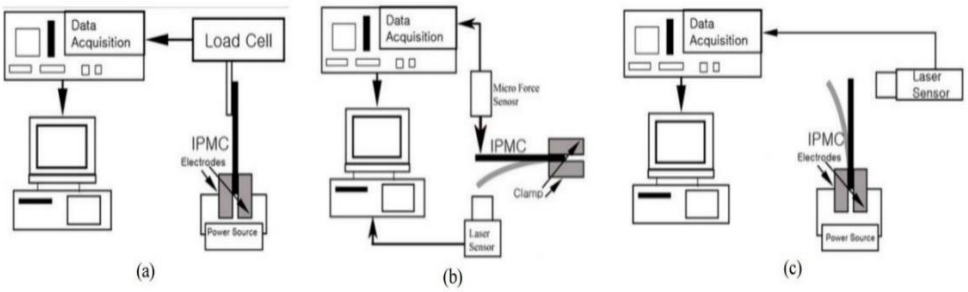

Figure 6: (a) Schematic diagram of blocking force test setup, (b) Experimental setup for stiffness measurement of IPMC actuator and (c) Schematic diagram of frequency response test setup [4]

1.3.1 Generative Force Analysis

Generative force, also named as block force, can be measured at the tip of IMPC, as displayed in **Figure 6(a)**. In test process, actuators would be block and load cell can be treated as sensor to measure block force directly. [14] The generative force mostly depends on thickness and mass of IPMC actuators in same voltage. However, only measure block force is far from enough, tip displacement and respond time are also important parameters in actuation.

1.3.2 Laser Vibrometry Analysis

In this system, one end of actuator is fixed while another is free. Laser can measure the tip displacement in real time because laser would reflect off form sample surface back to laser detector. Bending speed and respond time, meanwhile, can be calculated. Using this monitoring process, frequency response parament can be detected form 0.1 Hz to 200 Hz. [16]But it has limitation in

bending test. If sample bend out of the laser's viewing zone, data can not be obtained because rectilinear propagation of light.

1.3.3 Optical Imagery Analysis

Nowadays, a digital video optical system is used to measure the actuated bending. Recording is taken before application of the driving voltage. Video could intuitively reflect the dynamic process of bending. According to the video, most of parament, such as speed, bending angle, respond time, can be calculated easily. Even though optical imagery method is unable to detect in real time ionic EAPs generally use an optical analysis system for monitoring actuation behavior.

1.3.4 Capacitive Sensing

An alternative method to monitor actuation process is to measure the value change of capacitance. This method can be applied in almost dielectric elastomers. [17]Dielectric elastomer is a kind of *e*-EAP. It can be observed in large deformation (strain>100%) under high voltage (2.2-3 kV DC) because of Maxwell stresses. Capacitance for parallel plate capacitors is defined as **Equation 1.2.**

$$\mathrm{C} = \varepsilon_0 \varepsilon_r \frac{\boldsymbol{A}}{\boldsymbol{h}} \qquad (\mathbf{1.2})$$

Here, ε_0 is the permittivity of free space (which is a constant), ε_r is film's dielectric constant, A is the electrode area and h is sample thickness. According to this equation, capacitance will increase as thickness decreases or area increase in actuation process. The capacitive reactance can be obtained through a further calculation.

$$X_c = \frac{1}{\omega C} \qquad (1.3)$$

Where, ω is angular frequency of extra AC electric field. So, voltage change between input and output can be calculated using **Equation 1.4**:

$$V_{output} = \frac{R}{R + X_c} V_{input} \tag{1.4}$$

Through this method, there are two different electric fields applied on the dielectric elastomer samples: a driving DC voltage (2.2-3.0 kV DC) and a sensing AC voltage (300 Vpp AC at 100 Hz). It proved that this method is more suitable for *e*-EAP than *i*-EAP.

1.35 Current Electromechanical Actuation Model

To develop IPMCs, it is important to predict how they bend. Actuation process of IPMC can be fuzzy described some terms, such as slow steady and saturated. it is identical with human intuition. At first, bending need response time because most of movable ions distributed randomly in polymer matrix. And then, cations and anions begin to separate and accumulate at corresponding electrode with time going by. So, the rate of bending is nonlinear. Finally, IPMC reaches its maximum bending angle named saturated process because the number of ions in polymer is limited.

The actuation profile is nonlinear, with respect to time. Selection of the IPMC for designing actuators requires a clear understanding of bending mechanism.

Currently models can be divided by three parts:1) black box model, where based on test data rather than electromechanical mechanisms. 2) white box model, where both physical mechanisms and chemical processes can be considered. 3)

gray box model, which is taken bridge effect form black box model to white box model when the mechanisms are so complex that cannot explain process very well. [18]

1.35.1 White Box Model

White-box models, also named physics-based models, try to characterize the behavior of IPMC actuation. Kim, in 2008, proposed a relationship using for describing the diffusion of charges under electric field. [19]

$$\frac{\delta C}{\delta t} + \left(-D \bigtriangledown C - \frac{zDFC}{RT} \bigtriangledown \Phi\right) = -\bar{u} \bigtriangledown C \qquad (1.5)$$

Here, *C* is the concentration of charged particles, *D* is the diffusion constant, *Z* is the valence number, *F* is the Faraday constant, Φ is the electric potential, *R* is the universal gas constant, and $\bar{u}$ is the ionic velocity. It is assumed that all ions would move to their attracting electrode after extra filed applied. The model can fit results for Nafion base IPMC very well. [20]

The White Box Model also has shortcoming. The underlying physical and chemical mechanism of IPMC bending have not yet been totally understand. Additionally, the parameters of this equation are hard to detect.

1.35.2 Black Box Model

To explain IPMC bending process, Kanno et al developed a new model to fit experiment data in 1999. They treat IPMC sample as cantilever beam which fixed on end and another end is free. The fitting equation is shown as **Equation 1.6**.

$$Y(t) = Ae^{-\alpha t} + Be^{-\beta t} + Ce^{-\gamma t} + De^{-\epsilon t} + E \qquad (1.6)$$

Where, *A*, *B*, *C*, *D*, *E* and $\alpha, \beta, \gamma, \epsilon$ are constants which depend on bending behavior.

Physical processes and the mechanisms of IPMC deformation are not fully consider. A simpler black-box model was developed by Montazami in 2011. [21]

$$S(t) = S_{max}\left(1 - e^{\frac{-t}{\tau}}\right) \tag{1.7}$$

There are only two parameters: the maximum strain S_{max} and time constant τ. IPMC actuation follows a slow, steady and then saturated bending due to the flux of ions. So, the process is very similar with Arrhenius equation. However, the Montazami model can not fitting long time response or slow bending speed result.

1.35.3 Gray-Box Model

Gray-box models is a good fitting model which complex physical laws and empirical data. The mobile water molecules not be considered in gray-box model. Comparisons of how well gray-box models fit IPMC actuation data will be presented in **Chapter 3**. And, it will be shown that which model is most closely resemble the bending result.

According to gray-box model, the actuator can be divided by two part: electrical conversion and electromechanical conversion. In **Figure 7**,currents through resistances Re, R1 and Rn do not show any mechanical process, while the current through capacitive branches where the current is absorbed produces

the mechanical effect. It means that the current absorbed by capacitor is due to charges redistribution and generate stress inside the IPMC.

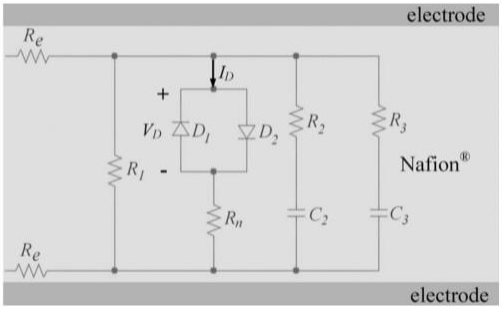

Figure 7:Equivalent electrical circuit for an IMPC-based actuator [22]

1.4 Back Relaxation

Back relaxation means that films begin to bend back to opposite direction after got maximin bending angle. Among them, some samples even back beyond the initial position. For commercial IPMC materials, different phenomena of back relaxation have been reported, which are showed in **Figure 8**.

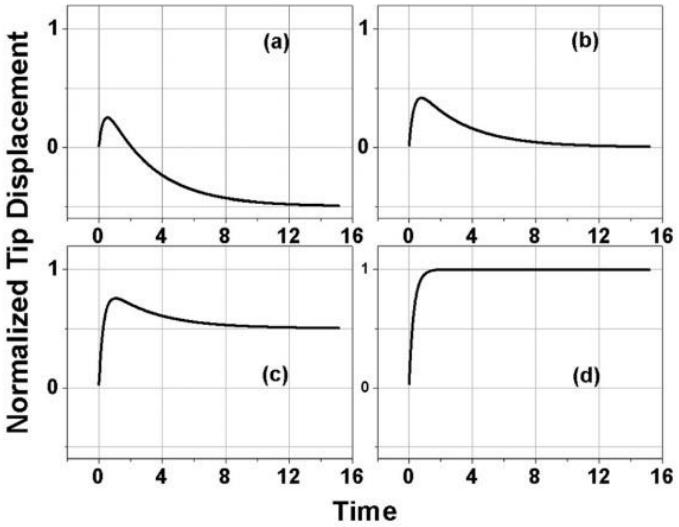

Figure 8:Different relaxation displacements of Nafion-IPMC under saturated conditions: (a)negative relaxation; (b) zero relaxation; (c) positive relaxation; and (d) no relaxation [23]

Nemat-Nasser claimed that Pt-Nafion–IPMCs doped with alkali cations show a large relaxation deformation beyond the initial position towards the cathode, as shown in **Figure 8(a)**.[1] Kim reported that bimetallic Pt-Pd electrode-based Nafion–IPMCs with various Pt-Pd ratios showed quite different relaxation phenomena, from negative relaxation in **Figure 8(a)** to no relaxation in **Figure 8(d)**. [2]In addition, Zhu and his co-worker show that Pd-, Cu-, and Ni-Nafion–IPMCs also show a large negative relaxation deformation like **Figure 8(a)**. However, Au-Nafion–IPMC often shows a positive deformation, as shown in **Figure 8(c)**. [3]

Shahinpoor et al. first pointed out that the back relaxation can be eliminated by removing some of the water content. [24]Shoji also found that the relaxation disappears at 50% relative humidity. [25]Scientists claim that there are three states of water in Nafion-base film at least: (1) water molecules closely bonded to the sulfonates; (2) loosely bound water; (3) free, unstrained, and bulklike water.(**Figure 9**) [23]So the different states of water molecules display different back relaxation phenomenon. Closely boned water relates to ions by chemical bonds. Some water molecules are weakly connected to closely boned water by hydrogen bond, which can rotate rather than move freely. There are several factors that influence the free water, such as the ions concentration, polymer machinal properties and size of the cluster. When relative humility decreases, the degree of freedom of all three states of water molecules is decrease.

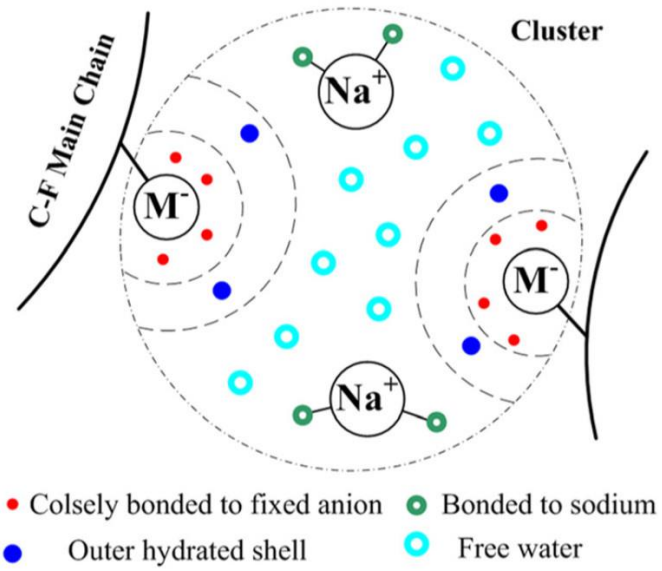

Figure 9: The three different states of water in IPMC [23]

The hydrated cations play a major role on back relaxation. Anode deformation is due to cation migration to cathode with water molecule, while the back relaxation is the result of hydrated cation go back driving by osmotic pressure [23]. In other words, the whole actuation process is mainly dependent on electrostatic stress and osmotic pressure. At first, the electrostatic stress is much higher than osmotic pressure. As the result, anode bending occurred. As approach the saturation bending, the motion of cations is finished, and hydrated cation begin to move to anode. The anode side of polymer will lose water lead to shrink. So, hydrated cations play a leading role in back relaxation.

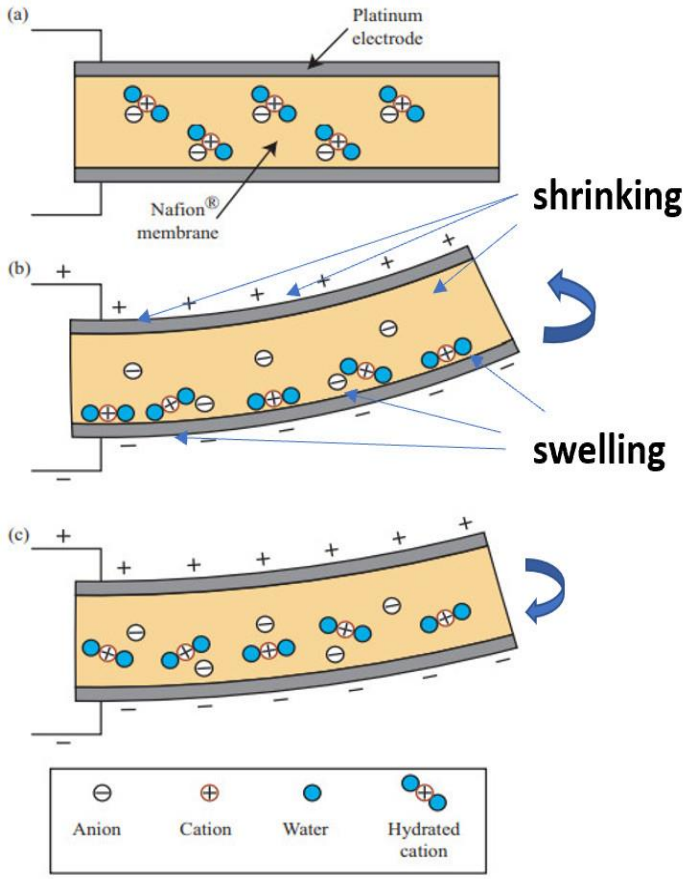

Figure 10:Shrinking and swelling of Nafion-base IPMC [26]

It is seen from the **Figure 11(a)** that films bend towards the anode because cations move to anode while anion fixed on the end of polymer branch chain after DC voltage applied (from a to b). After that, the strip slowly bends back to the cathode while electric field still applied (from b to c). When voltage off, the two metal electrodes would be shorted. The sample shows that bend towards the cathode (from c to d) immediately and then slow relaxed back to anode (from d to e). Finally, sample reaches a new equilibrium position after whole electromechanical actuation test.[27]

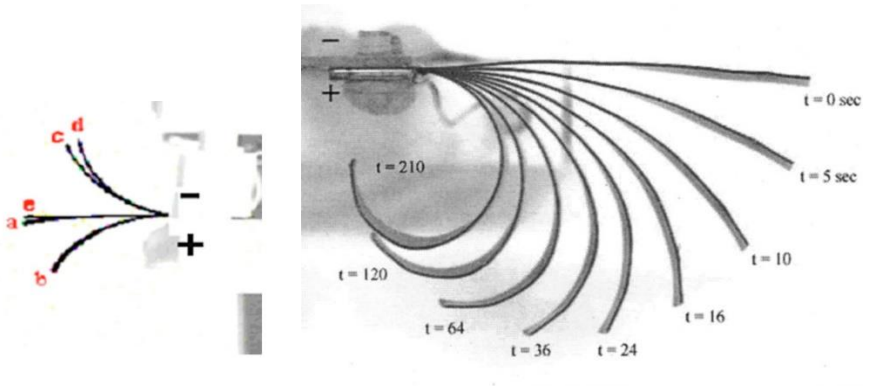

Figure 11：(a) Photos of a Nafion-base IPMC doping with alkali cations under 1.5V DC [27] (b) Photos of a Flemion-based IPMC doping with TBA^+, actuated by 3V DC [1]

For another common EAP material, Flemion-TBA^+ IPMC shows slowly bending speed without back relaxation (**Figure 11(b)**).

Back relaxation is harmful to engineering applications of IPMCs. The mechanism of back relaxation needs to study, and the problem is urgent to be solved.

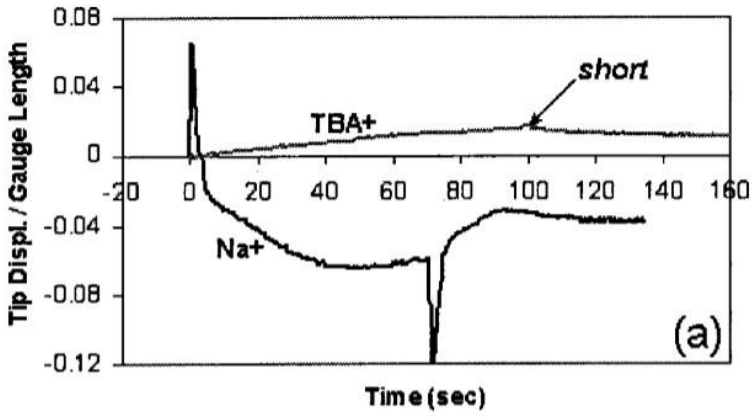

Figure 12:Actuation of a Nafion-based IPMC in Na^+ and TBA^+ form under a 1.5 V DC [1]

When ion species is the only variable, films doping with alkali cations are show obviously negative relaxation while Nafion-TBA IPMC shows slow bending without back relaxation. (**Figure 12**) Diameter of different cation is the

main reason. The size of tetrabutyl-ammonium (TBA^+) is much larger than that of alkali ions. [1]

In addition, Pd, Cu, Pt and Ni are coated as Nafion-IPMC's electrode also show a large negative relaxation deformation, while IPMC deposited Au as electrode often shows positive relaxation deformation. [4]When different metals coated on the surface of IPMC, morphology of electrode is different. It makes a great difference with surface resistance. If resistance high enough, sample does not show back relaxation. Negative relaxation occurs when surface resistance decreased. Lower surface resistance to produce the larger deformation and relatively stable actuation with positive relaxation phenomena.

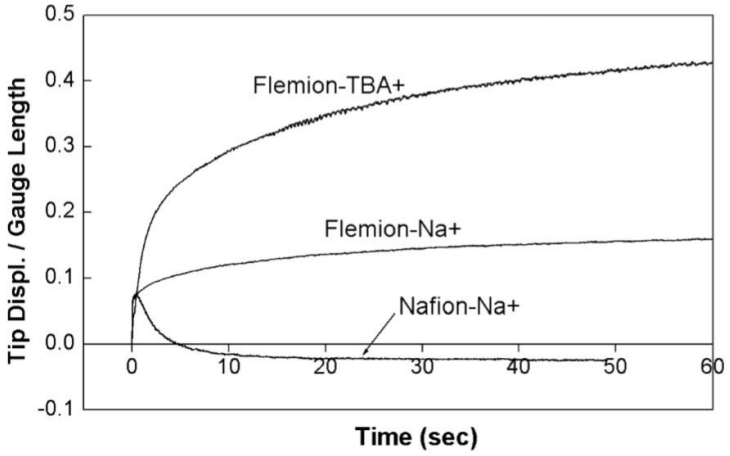

Figure 13:Actuation of a Nafion-based IPMC in Na^+ form and Flemion-base IPMC in Na^+ and TBA^+ under 1.5 V DC [1]

As for different polymer base, both Nafion- and Flemion-based IPMCs doping with Na^+ are bend towards the anode under 1.5V DC. Nafion-Na IPMC shows fast anode bending and then bend towards the anode until beyond initial state. While Flemion-based film shows stable positive bending without back relaxation. Different chemical structure of two polymer is the main cause of

back relaxation. There is a weak acid anion fixed at the end of side group of Flemion-base IPMC (**Figure 13**). Undissociated acid groups (–COOH) should be considered. It means that three chemical reactions occur in the polymer base at the same time. [23]

$$\mathrm{R-COONa} \rightarrow \mathrm{R-}COO^- + Na^+ \qquad (4.1)$$

$$\mathrm{R-COOH} \rightleftharpoons \mathrm{R-}COO^- + H^+ \qquad (4.2)$$

$$H_2\mathrm{O} \rightleftharpoons H^+ + OH^- \qquad (4.3)$$

The Na^+ is fully ionized. However, H^+ cation is not in Flemion-base film. When extra electric filed applied, all Na^+ and current H^+ move to cathode and therefore the concentration of H^+ is decrease near fixed anode. More and more H^+ will be generated from water molecule and then migrate to cathode. The slow secondary H^+ dissociation leads to slow anode deformation rather than back relaxation.

1.5 Motivation

After learned basic theories of EAPs, the research aims at developed a new type of IPMC, which property is low drive voltage, large strain, high reusability, controllable bending direction and short respond time. High efficiency test method, meanwhile, can be chosen to describe bending process in open air accurately. Furthermore, it is necessary to extend our knowledge to synthesis a new type of EAP materials.

Firstly, a new fluoro-polymer matrix film without branch chain need to be investigated, which has a lower glass transition temperature (Tg). Additionally, it is necessary to find a new way to doping ions to make sure concentration of cations and anions uniformly in polymer matrix. At the same time, physical electrode coating should be used to replace chemical electrode plating method. What's more, the new analysis method should be used to fitting larger angle bending.

1.6 Research Objective

1.61 Objective I- Development of New Materials for IPMC

The main targets of this research are developed a new linear polymer matrix which has high ionic mobility and large bending strain. As for metal ionic salt, the relatively large disparity of volume, between cations and anions, has effect on bending process.

Poly(vinylidene fluoride) (PVDF), a widely investigated solid electrolyte, is often served as ion-exchange membrane in cell industry. PVDF is a semicrystalline polymer. [28]According to different crystallization condition, PVDF can be divided into at least four different phases: the orthorhombic α，β and δ phase, and the monoclinic γ phase. **(Figure 14)** Among those, α-phase is nonpolar due to trans-gauche alternative conformation (TG^+TG^-). α-phase (a = 4.96 A_0, b= 9.64 A_0, c = 4.62 A_0, β = 900 A_0) is most steady orientation and it often obtained from the freezing process. [29]The strong polar β phase, which has all trans zigzag chain conformation (TTTT), has good pyro- and piezo-electric properties. β-PVDF (a= 8.58A_0, b= 4.91 A_0, c= 2.56 A_0) film is often

prepared by solution cast. [29]The weak polar δ phase, obtained from high temperature crystallization, has three trans linked with one gauche conformation ($TTTG^{+}TTTG^{-}$). When high extra electric field applied, the polar δ-PVDF can be obtained by polarizing form nonpolar α-PVDF. Several factors influence the crystal structure such as method of cast, solvent, stretching thin films and annealing process. Among them, β-PVDF is a very attractive polymer, widely used to piezoelectric sensors, energy storage devices and actuators. There is a significant dipole moment of each repeat unit. It means that a typical spontaneous polarization process is generated by additive dipole moments. [17]

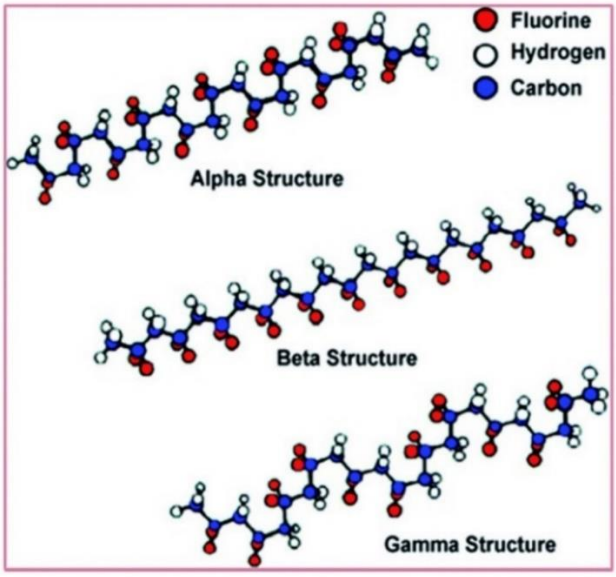

Figure 14:Diagrams of the chain conformation for α, β and γ crystalline phases of PVDF [30]

Because of PVDF excellent thermal stability, chemical resistance and hydrophobicity, films could be utilized in water treatment process, construction industry and fuel cell.

The glass transition temperature (Tg) of PVDF is -38℃, while the melting temperature is not fixed.[31] The Tg is defined as the temperature at which the polymer softens. Above Tg, PVDF exhibits rubber elasticity. It means that PVDF film is in a rubber state at room temperature. It means that chain segment can move freely but polymer molecule is fixed. As the result, the large strain can be generated. After the force is released, deformation can complete recovery.

Because there is no branched polymer chain can fix anions, both cations and anions moving freely in PVDF matrix. The PVDF film is able to absorb a larger amount of ionic salt without becoming noticeably softer compared to Nafion- or Flemion- base IPMC films.

1.62 Objective II: Development of an Efficient Electrode Plating Method

To coating a uniformly thin noble metal layer as compliance electrode, physical vapor deposition method should be used like vacuum evaporation and sputtering coating. The ionomer is sandwiched structure between two electrodes having large surface area that bear high levels of conductivity.

Compared to the chemical deposition of the gold coating, the physical electrode coating of PVDF is easier to handle and the time required for the coating is significantly reduced.

1.63 Objective III: Time-Dependent Electromechanical Actuation Analysis Model

The typical bending process can be divided by three processes: slow steady and saturated. By applying electric field, ions are attracted and begin to move to the corresponding electrodes. There is a respond time that cations and

anions form random distribution to directional migration. As time increases, more and more ions accumulate in the corresponding electrodes so that bending process is faster than before. Finally, ions could be saturated, and the bending angle reached maximum value. So, the relationship between bending process and time is worth studying.

Chapter 1 References

[1] Bar-Cohen Y, Zhang Q. Electroactive polymer actuators and sensors[J]. MRS bulletin, 2008, 33(3): 173-181.

[2] Bar-Cohen Y. Electroactive polymers: current capabilities and challenges[C] Smart Structures and Materials 2002: Electroactive Polymer Actuators and Devices (EAPAD). International Society for Optics and Photonics, 2002, 4695: 1-8.

[3] Bar-Cohen Y. Artificial muscles using electroactive polymers[M] Biomimetics. CRC Press, 2005: 285-308.

[4] Bhandari B, Lee G Y, Ahn S H. A review on IPMC material as actuators and sensors: fabrications, characteristics and applications[J]. International journal of precision engineering and manufacturing, 2012, 13(1): 141-163.

[5] Bar-Cohen Y. WorldWide Electro Active Polymers[J]. 1999.

[6] Cheng Z, Zhang Q. Field-activated electroactive polymers[J]. MRS bulletin, 2008, 33(3): 183-187.

[7] Xu, T.-B., Z.-Y. Cheng, and Q. Zhang, High-performance micromachined unimorph actuators based on electrostrictive poly (vinylidene fluoride–trifluoroethylene) copolymer. Applied physics letters, 2002. 80(6): p. 1082-1084.

[8] Cheng, Z., et al., Design, fabrication, and performance of a flextensional transducer based on electrostrictive polyvinylidene fluoride-trifluoroethylene copolymer. Ultrasonics, Ferroelectrics and Frequency Control, IEEE Transactions on, 2002. 49(9): p.1312-1320.

[9] Shahinpoor, M., Ionic polymer–conductor composites as biomimetic sensors, robotic actuators and artificial muscles—a review. Electrochimica Acta, 2003. 48(14): p. 2343-2353.

[10] Mauritz, K.A. and R.B. Moore, State of understanding of Nafion. Chemical reviews, 2004. 104(10): p. 4535-4586

[11] Zhenyi M, Scheinbeim J I, Lee J W, et al. High field electrostrictive response of polymers[J]. Journal of Polymer Science Part B: Polymer Physics, 1994, 32(16): 2721-2731.

[12] Pelrine R, Kornbluh R, Pei Q, et al. High-speed electrically actuated elastomers with strain greater than 100%[J]. Science, 2000, 287(5454): 836-839.
[13] Kim K J, Shahinpoor M. Ionic polymer–metal composites: II. Manufacturing techniques[J]. Smart materials and structures, 2003, 12(1): 65.
[14] Akle, B.J., M.D. Bennett, and D.J. Leo, High-strain ionomeric–ionic liquid electroactive actuators. Sensors and Actuators A: Physical, 2006. 126(1): p. 173-181.
[15] Nemat-Nasser S, Wu Y. Tailoring the actuation of ionic polymer–metal composites[J]. Smart Materials and Structures, 2006, 15(4): 909.
[16] Xiao, Y. and K. Bhattacharya. Modeling electromechanical properties of ionic polymers. in SPIE's 8th Annual International Symposium on Smart Structures and Materials. 2001.International Society for Optics and Photonics.
[17] Jung, K., K.J. Kim, and H.R. Choi, A self-sensing dielectric elastomer actuator. Sensors and Actuators A: Physical, 2008. 143(2): p. 343-351.
[18] Kanno, R., et al. Characteristics and modeling of ICPF actuator. in Proceedings of the Japan-USA symposium on flexible automation. 1994.
[19] Kim, K., et al. Ionic polymer-metal composite: an emerging smart material. in World Forum on Smart Materials and Smart Structures Technology: Proceedings of SMSST'07, World Forum on Smart Materials and Smart Structures Technology (SMSST'07), China,22-27 May, 2007. 2008. CRC Press
[20] Pugal, D. et al. A self-oscillating ionic polymer-metal composite bending actuator. J. Appl. Phys. 103, 084908–084906 (2008)
[21] Montazami, R., et al., Thickness dependence of curvature, strain, and response time in ionic electroactive polymer actuators fabricated via layer-by-layer assembly. Journal of pplied Physics, 2011. 109(10): p. 104301.
[22] Moeinkhah H, Rezaeepazhand J, Akbarzadeh A. Analytical dynamic modeling of a cantilever IPMC actuator based on a distributed electrical circuit[J]. Smart Materials and Structures, 2013, 22(5): 055033.
[23] Zhu Z, Chang L, Asaka K, et al. Comparative experimental investigation on the actuation mechanisms of ionic polymer–metal composites with different backbones and water contents[J]. Journal of Applied Physics, 2014, 115(12): 124903.
[24] Shahinpoor M, Kim K J. Ionic polymer–metal composites: III. Modeling and simulation as biomimetic sensors, actuators, transducers, and artificial muscles[J]. Smart materials and structures, 2004, 13(6): 1362.
[25] Shoji E, Hirayama D. Effects of humidity on the performance of ionic polymer− metal composite actuators: experimental study of the back-relaxation of actuators[J]. The Journal of Physical Chemistry B, 2007, 111(41): 11915-11920.

[26] Fleming M J, Kim K J, Leang K K. Mitigating IPMC back relaxation through feedforward and feedback control of patterned electrodes[J]. Smart Materials and Structures, 2012, 21(8): 085002.
[27] Nemat-Nasser S, Zamani S, Tor Y. Effect of solvents on the chemical and physical properties of ionic polymer-metal composites[J]. Journal of Applied Physics, 2006, 99(10): 104902.
[28] K. Tashiro, “Crystal Structure and Phase Transition of PVDF and Related Copolymers,” In H. S. Nalwa, Ed., Ferroelectric Polymers Chemistry, Physics and Applica- ons, Marcel Dekker, New York, 1995, pp. 63-180.
[29] Gregorio Jr R, Borges D S. Effect of crystallization rate on the formation of the polymorphs of solution cast poly (vinylidene fluoride) [J]. Polymer, 2008, 49(18): 4009-4016.
[30] Wan C, Bowen C R. Multiscale-structuring of polyvinylidene fluoride for energy harvesting: the impact of molecular-, micro-and macro-structure[J]. Journal of Materials Chemistry A, 2017, 5(7): 3091-3128.
[31] Rogers J A, Carr D W, Bogart G R. Fabrications of PVDF gratings: final report for LDRD project 79884[R]. Sandia National Laboratories, 2005.

Chapter 2： Experimental Setup and Procedure

2.0 Research Methodology and Measurement Process

To realize the previous objectives, the detailed research and measurement are presented in this chapter. This thesis had chosen the PVDF as the object of study because its low glass transition temperature and good mechanical property. Perchlorate salts were doped in PVDF solution. The composite film was prepared by casting form DMF. Glass side was used as substrate for solution cast. After film dry, using tweezers to peel off film from glass side. The ionomer film could be cut into desirable shape. The chain conformation has been determined by X-ray diffraction. Employing differential scanning calorimetry (DSC), the melting and crystallization process of PVDF ionomer were investigated. The crystallinity and melting point could be calculated at the same time.

Nobel metal such as 30-nm thick gold was deposited on the top and bottom sides as electrode. The physical vapor deposition was easy to control the thickness of electrode. After that, dielectric property, such as permittivity, loss and relaxation time, could be measurement by impedance analyzer. Using self-made instrument test bending process. The DC filed was generated by using Function Generator. A digital video optical system was used to record the whole actuation process. Measurements were taken after voltage on. According to record data, bending angle and strain can be obtain by Tracker software and Newton’ s method. Humid air could be pumped in to system to control

atmospheric humidity So, both electromechanical and dielectric test would be accomplished.

2.1 Material Preparation

PVDF power (M_w~534,000) and perchlorate salts, such as lithium perchlorate (LiP), copper perchlorate (CuP) and cobalt perchlorate (CoP), were obtained from Sigma-Aldrich chemistry company.

PVDF composite solutions were created using 0.3g of solute in 20ml N,N-dimethyl-formamide (DMF), which the concentration of ionic salt is 15wt.%. PVDF matrix had able to hold large number of ions and do not block cation and anion diffusion. A clean homogeneous solution was created by magnetic stir for 12h and stand more than 12h. Glass side was used for solution cast before solution cast. Glass side need preheat in oven before casting.8ml PVDF-based solution were dropped by Fisherbrand 100-1000μL Finnpipette. The solution was kept in 40℃ for almost 3h. After totally dry, films were peeled off form glass side. It was necessary to cover another glass side to make film flat. As for thickness measurement, Mitutoyo 543-252 Absolute Digimatic Indicator was used, which resolution was 1 μm. A thin noble metal layer, 20-30nm gold, was deposited on top and bottom sides of film as electrode. The rectangle sample was cut into 19.10×6.35 mm, which was used to actuation test and dielectric property test.

2.2 Characterization and Measurement

This part will highlight the details of test process and new analysis method, which are different form previous work. New software and self-made chamber are utilized in my research.

2.2.1 Actuation Excitation Overview and Procedure

A quantitative static and dynamic performance evaluation system is developed (**Figure 15**).

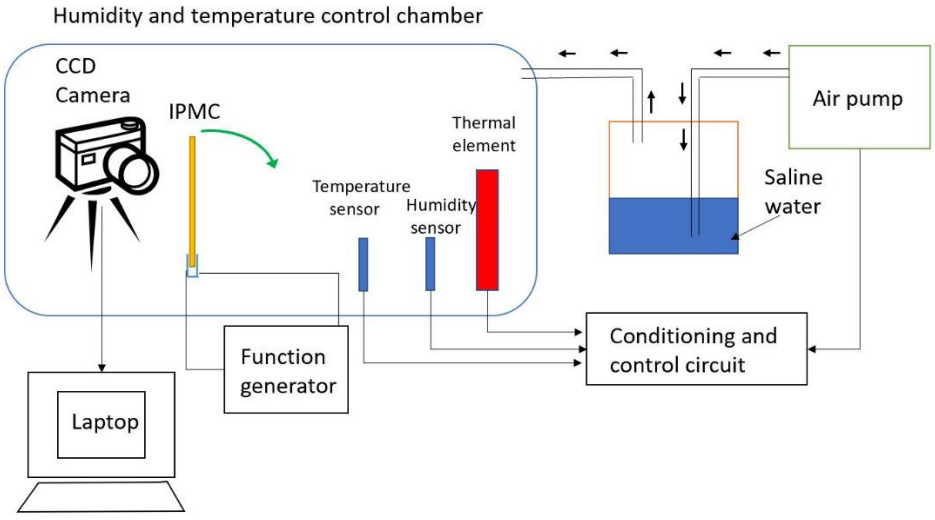

Figure 15:The diagram of new monitoring system

The bending process is the best manifestation of actuator property. Even though the bending speed of sample under 10V DC is faster than at 4V DC, the lower voltage drive large stain is a research trend. So, all of samples were tested in 3~4V DC voltage range. Four or five small rectangle samples cut from one whole film. Samples would bend under constant DC voltage until blocked by the clip. After that reverse voltage was applied to straighten the film back to initial

state. IPMC samples were tested twice or three times under a constant DC voltage with their bending data bending averaged.

To realize large stain, more ions should be infused into polymer matrix as charge carriers. But excess ionic salts are added into polymer film, the crystallinity would decrease. As the result, the film becomes softer and hard to control. [1]

According to previous work, 15 wt.% of ionic salts not only provide enough movable cations and anions but also show maximum bending angle in first 1min. Therefore, 15wt. % and 3~4V DC were chosen in following research. PVDF was treated as polymer matrix. Additionally, humidity was controlled during testing using an AC-9901 air pump. Because ambient humidity was a variation in the range of 20%~ 50% in different time. Air was pushed through a saturated sodium-chloride salt solution and then into the incubator. The incorporation of this device enabled a constant humidity within the testing chamber that ranged between 20-45%.

2.2.2 Characterization of Sample Dielectric Properties

Dielectric properties can be measured using Agilent 4294A Impedance Analyzer. Its frequency range is 100~1MHz during the impedance test process. It is noteworthy that AC voltage is so small that had little effect on actuation bending.

2.2.3 Optical Analysis Procedure

Bending process is taken as my research object rather than block force (output force). It is important to select suitable method to monitoring the

actuation of IPMC. Traditional test method is relied on laser and camera. As conduction time goes on, tip displacement can be measured. If large strain or crimp occurs, samples will beyond the detection area. So, a new way of monitoring bending process and analyzing the actuation data should be developed.

As stated earlier, the laser rangefinder has a great limitation, a CCD camera or digital smart phone are considered. Lens face to thickness dimension of rectangle sample and camera record whole bending process including back relaxation. After that, video need analysis using a software named Tracker. The basic procedure of analysis includes establish coordinate, building tracing points and obtaining Excel report. The next part will give more detailed interpretation of iterative data got form Tracker. But it is not a real-time monitoring method.

2.2.4 XRD Equipment and Differential Scanning Calorimetry

As mentioned previously, PVDF exists at least four different phases. Phases of thin films were analyzed by X-ray diffractometer, using Cu Kα radiation, with the generator working at 40kV and 40mA. Test angle range (2θ) is 10~30°. Scan angle of each step is 0.1° and scan speed is 10s/step. Diffraction only occur in a few specific directions, determined by Bragg's law:

$$2d\sin\boldsymbol{\theta} = n\boldsymbol{\lambda} \tag{2.1}$$

Where d is the spacing between two parallel atomic planes and the θ is the incident angle. The value of d-spacing is different with different crystal structure. So different phases have different diffraction angles. The characteristic peaks of α-phase are 17.94° (100), 20.2° (021), 29.92° (110), 36.12 ° (200) and 39 ° (002). γ-phase peak at 18.5° (020),20.1° (110),26.8° (002) and 38.7° (211) respectively. Peaks at 20.7° (200) and 20.8° (110) confirm the existence of β-

phase in PVDF, other peaks would locate in 36.6° (020) (101) and 56.9° (221). [2]

Another experimental technique used in PVDF samples is differential scanning calorimetry (DSC). This technology can measure the heat differentness between sample and reference when phase transition occurs no matter first-order or second-order phase transition. At the same time, other properties of polymer like glass transition temperature (Tg), melting temperature (Tm) and crystallization temperature (Tc) can be detected. For the melting process, the area of melting peak is the enthalpy (heat) absorbed in melting process. So, crystallinity can be calculated using by following equation.

$$\mathrm{C} = \frac{\Delta H}{\Delta H_{100\%}} \tag{2.2}$$

where $\Delta H_{100\%}$ is the heat of fusion for 100% crystalline. However, different phases of PVDF have different value of heat of fusion for 100% crystallin. According to theoretical calculation, the heat of fusion of main two phases are ΔH_α = 104.5 J. g^{-1} and ΔH_β = 219.7 J. g^{-1} respectively. [3,4] In my reach, used an aluminum (Al) pan to weigh sample (mass range: 8-12mg) which is already cut into pieces, while another Al pan is empty which can be regarded as reference. The heating and cooling rate are 5℃/min and the heating range from 60℃ to 200 ℃.

There are many factors can influence on crystallinity of polymer, such as annealing treatment, stretching and nucleating agent.

2.3 Data Analysis Calculation

This part will briefly introduce the iterative method of process video data. Assumptions need be established to solve the equation at the same time. It is necessary to discuss the principle and process of iteration in following part.

2.3.1 Radius of Curvature, Tip-Displacement Angle, and Determination of Electromechanical Strain

In Tracker software, the initial length of sample can be measured after reference system established. When extra electric filed applied, the trajectory of tip can be tracked. Bending process can be divided by many frames. For each frame, the coordinate value can be obtained. The track process is automatically from one frame to next frame. A series of coordinate value are conculcated in Excel. According to those data, the chord length can be calculated by Pythagorean theorem. It is reasonable to assume that the bending process showed a near-perfect circular curve. The initial length of sample equates to length of arc, as displayed in **Figure 16**.

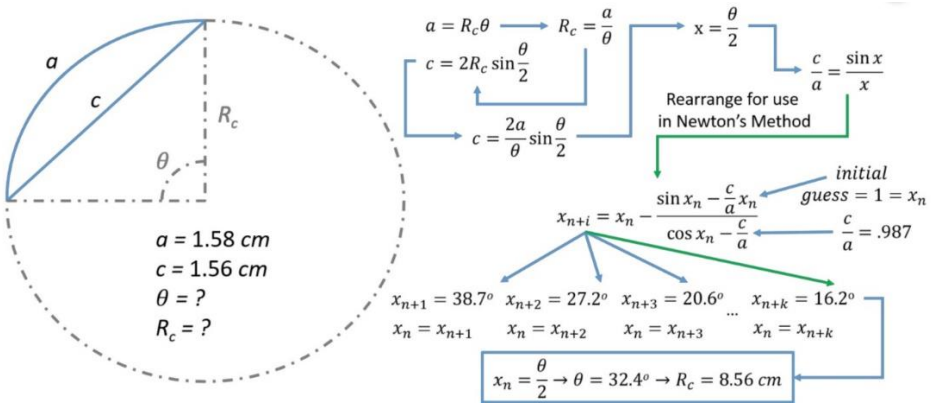

Figure 16:Newton's Method Process

To calculate the bending angle, only two known quantities, which are the arc length (a) and the chord length (c), are far from enough. According to

geometry, there are two basic equations can be obtained. Unfortunately, the value of *Rc* cannot be calculated directly only based on a and c. Newton's Method is a way of solving the problem.

$$\mathrm{a} = R_c\,\theta \tag{2.2}$$

$$\mathrm{c} = 2R_c \sin\frac{\theta}{2} \tag{2.3}$$

Newton's Method, which is a way for root-finding algorithms, is chosen solve problem. R_c can be calculated using **Equation 2.3**. Adopting following of forms to iteration.

$$x_{n+1} = x_n - \frac{f(x_n)}{f'(x_n)} \tag{2.4}$$

Where X_n is an initial guess for a root of *f(x)*, X_{n+1} is a next approximation which is closer to real value. If the function *f(x)* satisfies the assumptions made in the derivation of the formula, the process will repeat until a sufficiently accurate value is reached. The function *f(x)* can be obtained by combing **Equation 2.2** and **Equation 2.3**, yielding:

$$\mathrm{c} = \frac{2a}{\theta}\sin\frac{\theta}{2} \tag{2.5}$$

$$\frac{c}{a} = \frac{\sin x}{x} \tag{2.6}$$

Where, $x = \frac{\theta}{2}$. Rearranging this function into an equality:

$$f(x) = \sin x - \frac{c}{a}x \tag{2.7}$$

The function's derivative $f'(x)$ is:

$$f'(x) = \cos x - \frac{c}{a} \tag{2.8}$$

The process is repeated as:

$$x_{n+1} = x_n - \frac{\sin x_n - \frac{c}{a}x_n}{\cos x_n - \frac{c}{a}} \tag{2.9}$$

According to **Equation 2.9**, an initial guess (X_0) is between 0 and 2π. For the simplicity iteration, it is assumed that initial guess is 1 radian. After ten times iteration, the value of root is stably. Based on angle value, the radius of curvature (R_c) can be obtained. The bending angle θ increase with the decreasing of radius of curvature (R_c) with conduction time prolonged. The geometric relationship of bending process is displayed in **Figure 17**.

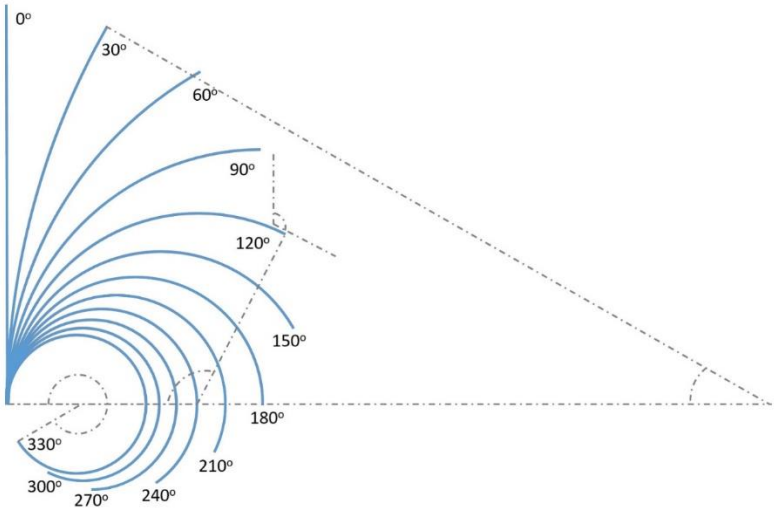

Figure 17: Progression of EAP bending angle θ and radius of curvature (R_c)

Furthermore, strain can be calculated using **Equation 2.10**. [5]

$$S = \frac{h}{2R_c} \tag{2.10}$$

Where h is sample thickness. The strain of EAP is inversely related to the radius of curvature (R_c). It is clear that the smaller of radius of curvature due to larger bending angle thus greater strain.

2.3.2 Dielectric Calculations and Analysis

As mentioned earlier, a CCD camera can record the whole bending process of IPMC under constant DC voltage. In this part, a new research method would be presented. Frequency-dependent dielectric properties are taken into consideration. Impedance analyzer can directly measure the capacity (Cp) and loss (D) using Cp~D mode.

As an example, the dielectric property plots of pure PVDF film are displayed in **Figure 18**. The test frequency ranges from 100 Hz to 1M Hz.

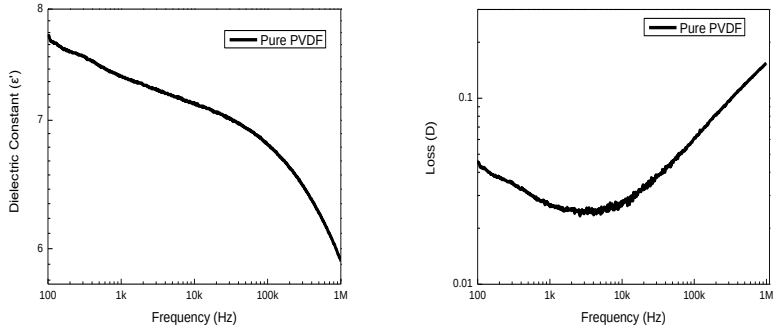

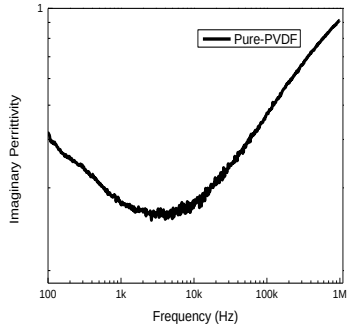

Figure 18: Example of dielectric calculations for a film of Pure PVDF films showcasing the a) real permittivity, b) loss and c) imaginary permittivity

Chapter 2 References

[1] Zhang, Y., et al., Effects of lithium perchlorate on poly (ethylene oxide) spherulite morphology and spherulite growth kinetics. Journal of Applied Polymer Science, 2012.123(4): p. 1935-1943

[2] Li W, Meng Q, Zheng Y, et al. Electric energy storage properties of poly (vinylidene fluoride) [J]. Applied Physics Letters, 2010, 96(19): 192905.

[3] Nakagawa, K.; Ishida, Y. J. Polym. Sci. Polym. Phys. Ed. 1973, 11, 1503. [26] Yu, L.; Cebe, P. Polymer 2009, 50, 2133.

[4] Gradys A, Sajkiewicz P. Determination of the melting enthalpy of β phase of poly (vinylidene fluoride) [J]. e-Polymers, 2013, 13(1).

[5] Zhang, Q., et al., An all-organic composite actuator material with a high dielectric constant. Nature, 2002. 419(6904): p. 284-287.

Chapter 3 Development and Analysis of a PVDF-Base IPMCs

3.0 Overview

As mentioned in **Chapter 1**, the principle of IPMC actuator bending was the diffusion of ions under electric field. For my sample, both cations and anions could move free in solid PVDF electrolyte. Additionally, how to prepare the PVDF-base samples was already discuss in previous chapter. The lithium perchlorate, copper perchlorate and cobalt perchlorate were choice to doping into PVDF film. Simultaneously, same number of cations films were prepared and tested them under in same context. Similarly, same number of anions films were synthesized to figure out different number of Li^{+} and Co^{2+} effect on bending strain and direction. This chapter will discuss the effect of different cations doping in matrix and emphatically analyses the actuation behavior of PVDF-CoP films.

3.1 Physical Parameters of PVDF-CoP Film

3.11 Research on the Phase of PVDF-CoP Film

In **Figure 19**, the signal intensity peak is observed at 20.8° (2θ values), which are belongs to β-phase. This is because all films were cast from solution and the carboxyl of glass side will help β-phase crystallizing.

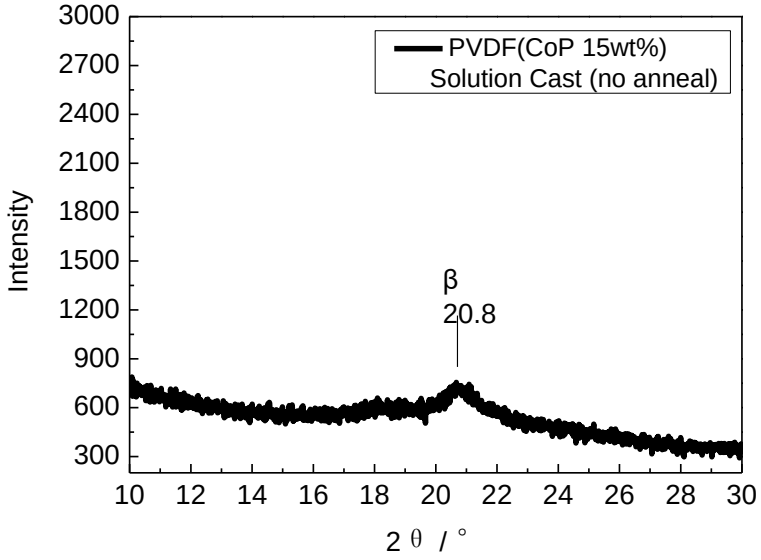

Figure 19:XRD spectra data of PVDF doped with 15 wt.% CoP

3.12 Measurement of Crystallinity and Temperature of Melting and Crystallization of PVDF-CoP Film

Figure 20(a) displays DSC curve of pure PVDF film. The peak of melting temperature is 169.90℃. While the peak of crystallization temperature is 145.02℃. According **Equation 2.2,** the crystallinity of pure PVDF film casted form solution is 34.93%.

Presented in **Figure 20(b)** is the DSC curve of PVDF film doped with 15 wt.% CoP. Melting temperature and crystallization become smaller. The crystallinity is decrease to 32.04%. When enthalpy is constant, the melting temperature will decrease. Because the entropy of composite will increase after doping.

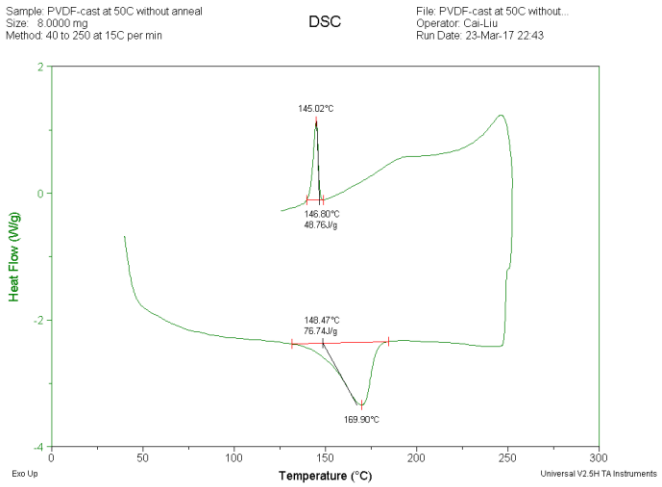

(a)

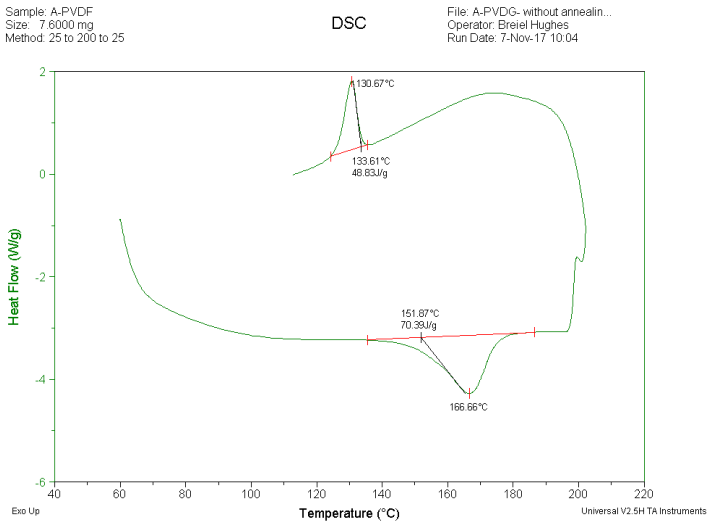

(b)

Figure 20:DSC curves of a) pure PVDF film and b) PVDF with 15 wt.% CoP

3.13 Dielectric Analysis of PVDF-CoP Film

This part is devoted to systematic study of frequency-dependence dielectric respond under AC extra field. It means that dielectric properties change before and after doping with perchlorate. Impedance analyzer would be used to test the film's dielectric properties in open air. The frequency of AC field is from 100 Hz to 1MHz.

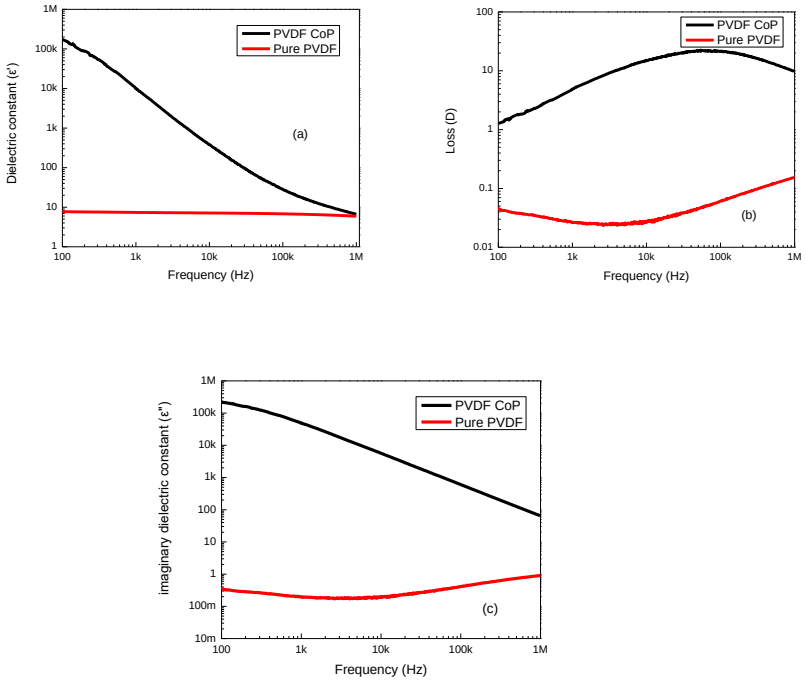

Figure 21:Frequency dependent a) real permittivity, b) dielectric loss and c) imaginary dielectric constant in 43% relative humidity at 20℃

It is clear that all of dielectric properties are increase obviously after doping with CoP in low frequency range. (**Figure 21**) It means that PVDF-CoP IPMC is an ionic conductor. Additionally, the loss peak shifts to higher frequency direction. In high frequency, the intrinsic characteristics of PVDF is showed. The oscillate of dipoles of β-PVDF is dominate rather than ions motion. **Table 2** list these dielectric parameters and the values where the loss peak is present.

Table 2:Frequency-dependent dielectric data for PVDF-based IPMC

Sample	Approximate values				At Loss Peak Frequency			
	ε′ (100Hz)	D (100Hz)	ε′ (1MHz)	D (1MHz)	*F* (kHz)	ε′	D	ε″
Pure PVDF	7.74	0.04	5.91	0.15	2.61	7.27	0.02	0.17
PVDF-Cop	$1.75E^{+05}$	1,28	6.62	9.74	53.88	49.01	22.5	74.82

3.2 Actuation Performance (Strain and Tip-Angle Displacement)

The main reason of the IMPC films actuation is that the size difference between cation and anion. Both cation and anion will redistribute after extra electric filed applied. Cations are attracted to move to cathode, while anions are forced to migrate to anode. More and more ions accumulate to respective electrode with the time goes by. As the result, different pressures are generated between cathode and anode. It is clear that expansion and decrement are created lead to macroscopic bending.

In my experiment, cobaltous perchlorate (CoP), copper perchlorate (CuP) and lithium perchlorate (LiP) are treated as doping agent. The diameter of different ions is showed in **Table 3**. [1]

Table 3:Diameter of different ions

Ions	Atomic Number	Valence	Diameter(Å)	Hydrated(Å)
Li^{+}	3	+1	0.76	3.82
Co^{2+}	27	+2	0.74	4.23
Cu^{2+}	29	+2	0.73	4.19
ClO_4^{-}	-	-1	2.40	-

After doping, the proposed modes of bending included ionization totally, ions can move freely, the velocity of ions drift is constant, ionic hydration does not occur and ions would accumulate at the interface between matrix and electrode finally. Let us take PVDF-CoP IPMC as an example, **Figure 22** shows the whole process of ions redistribution and accumulation of

PVDF-CoP IPMC. The mechanism of PVDF-CuP sample is similar because closer relative atomic mass and diameter of cation.

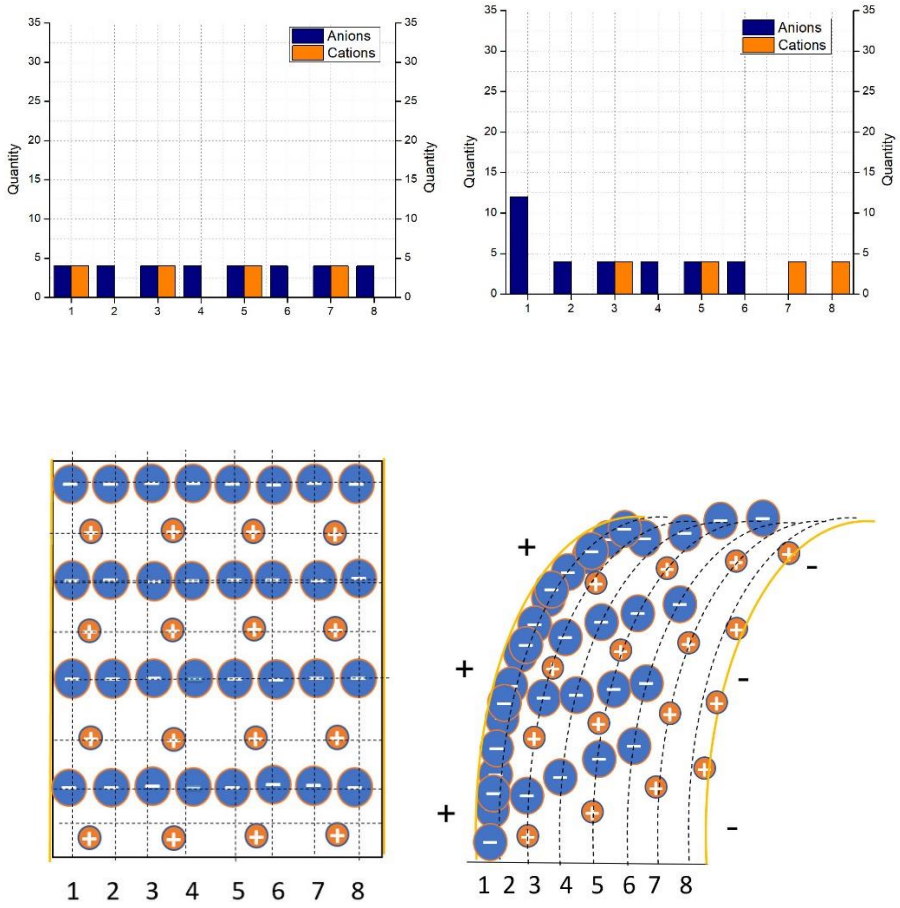

(a) (b)

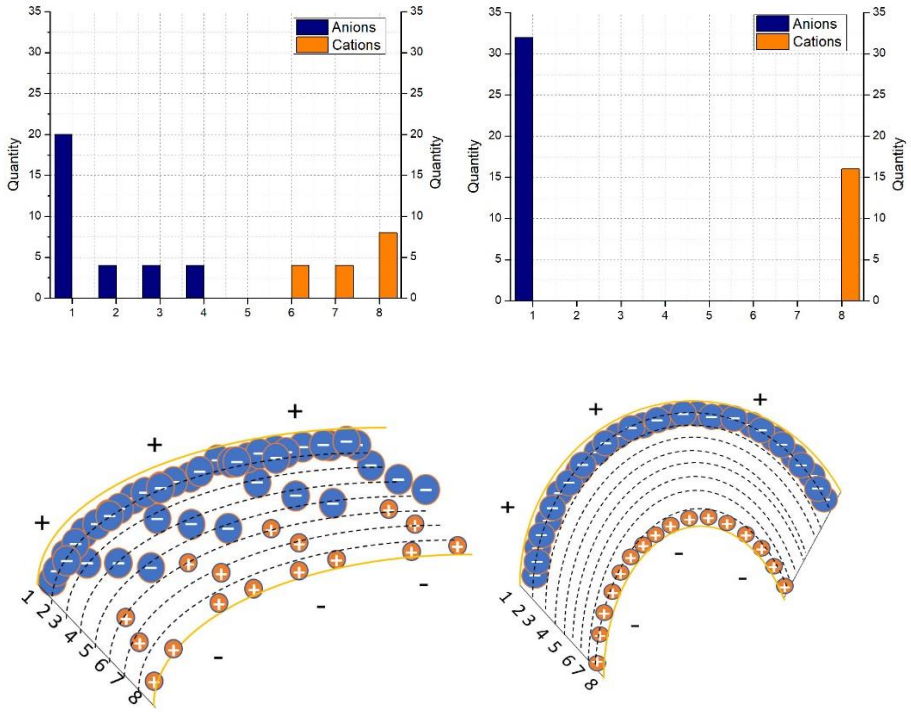

(c) (d)

Figure 22: The process of ions accumulation of PVDF-CoP IPMC under DC electric filed. a) T=0s b) T=T1 c) T=T2 d) T=T3

Through inspection of **Figure 22. a-d**, ions are attracted to move and accumulate at corresponding electrode sides. At first, cation and anion distributed randomly and uniformly in PVDF matrix, shown in **Figure 22(a)**. There is no expansion or constriction on each side of IPMC. By applying electric field, ions begin to move (**Figure 22(b)**). With the time going, the ions separate completely (**Figure 22(c)**). Finally, all of ions are accumulate at corresponding electrode sides (**Figure 22(d)**). The sample experience expansion due to different size of cation and anion accumulate at different sides. To be specific, big anions accumulate at anode while small cations get together on cathode, together with the quantity of anions is double that of cations. So, anode

side of IPMC shows expansion while cathode side displays constriction. For bulk sample, it is shows obviously cathode deformation.

3.3 Variable-Voltage Testing of PVDF-CoP IPMCs

The actuator is tested under varying voltages to obtain what is lowest drive voltage. **Figure 23** displays that PVDF-CoP IPMC curves under 3V,3.5V and 4 V DC, which represent response of the actuation without any fitting. The exhibits, however, are not at all exposed at different DC voltages. The bending angle is smallest, and the response time is longest when 3V DC applied. When the samples are actuated under 3.5V and 4V, the actuation angle and response time are almost same. It is clear evident that bending occurs under the voltage rang 3~4V and actuation speed increase with voltage increasing. It means that the bending performance determine by extra DC voltages when the concentration of ions is same. 3V is lowest drive voltage and 4V is the highest electromechanical efficiency for PVDF doping with 15wt.% Cop IPMC. If high voltage (>4V DC) applied for a long time (>1min), permanently deformation easy occurs although bending speeding is very fast.

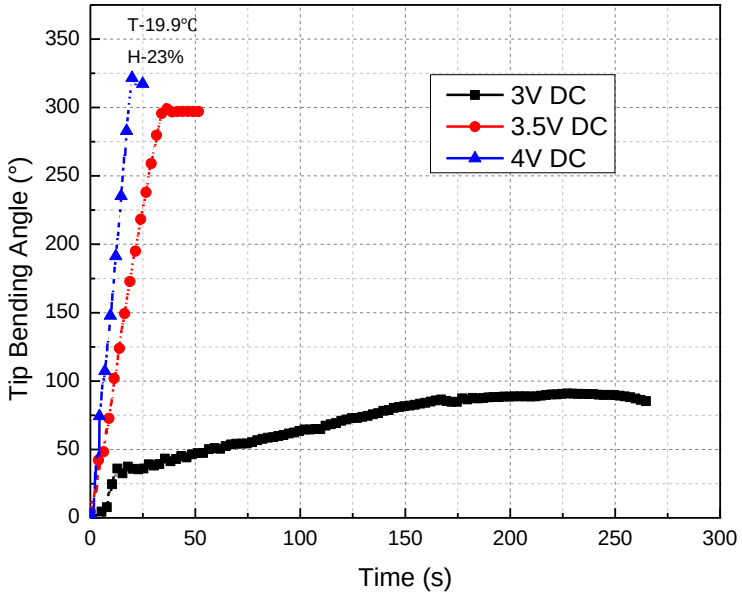

Figure 23: Results for varying voltage testing for 15wt.% Cop

3.4 Variable-Ions Testing of PVDF-Base IPMCs

In my research, IPMCs doping with different cations bend toward different direction. PVDF-LiP IPMC shows anode deformation while PVDF doping with Co^{2+} and Cu^{2+} show cathode deformation. Unlike other commercial Nafion-base IPMCs, PVDF-CoP is the first one of active polymer which shows large cathode deformation. The diameter of cations has little difference, whereas the bending angle and strain exists significant difference. This is because that the quantity of Li^{+} is two times than that of Cu^{2+} and Co^{2+} to make sure the number of anions is constant. Transition element Cu and Co are observed to contrast and analyze because of the similar relative atomic mass and size.

PVDF-ions Composites	T (s)	θ_{max} (°)	S_{max} (%)
15 wt.% Cop	20	324	0.37
15 wt.% Cup	28	270	0.34
8.7 wt.% LiP (Same anions) (Double cations)	30	170	0.20

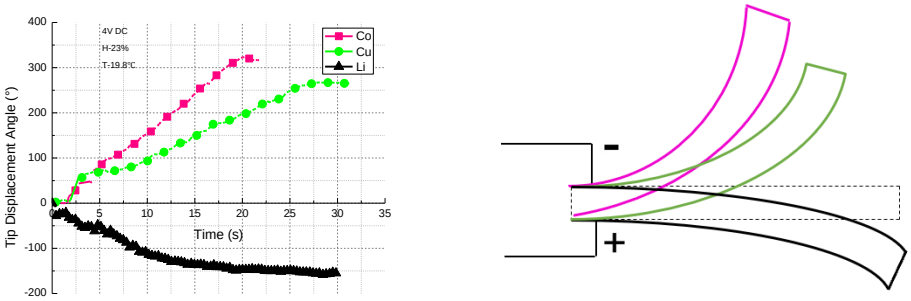

Figure 24:Actuation plot for PVDF-based IPMCs doping with Co^{2+}, $Cu^{2+}$and Li^{+}, under 4V DC

Table 4:The paraments of bending for PVDF-base samples doping with different cations under 4v DC

Large actuation under 4 V have been implemented for PVDF IPMC doping with CoP, CuP and LiP at low-humidity atmosphere (23%) and room temperature, as display in **Figure 24**. For 4V DC voltage, the bending speed of PVDF-CoP film is faster than that of PVDF-CuP. Over 250° of bending angle and less than 30s response time are observed. Because the two different ions

have almost the same dimension, relative atomic mass and valence. The mechanism of bending is already shown in **Figure 22**.

As for PVDF-LiP IPMC, samples bend to anode side. So, ions accumulation model which try to explain IPMC actuation is incomplete correct. The process of ionic hydration should be taken account because the diameter of hydrated cation is larger than bare cation. Together with the quantity of cation and anion is equal. Although ionic hydras ability of lithium is low, the diameter of anions is smaller than that of hydrated cation. (**Figure 25**) It is the reason why PVDF-LiP IPMC bend to opposite direction. But the tip bending angle is inferior to that of PVDF-CuP and PVDF-CoP IPMC (<180°).

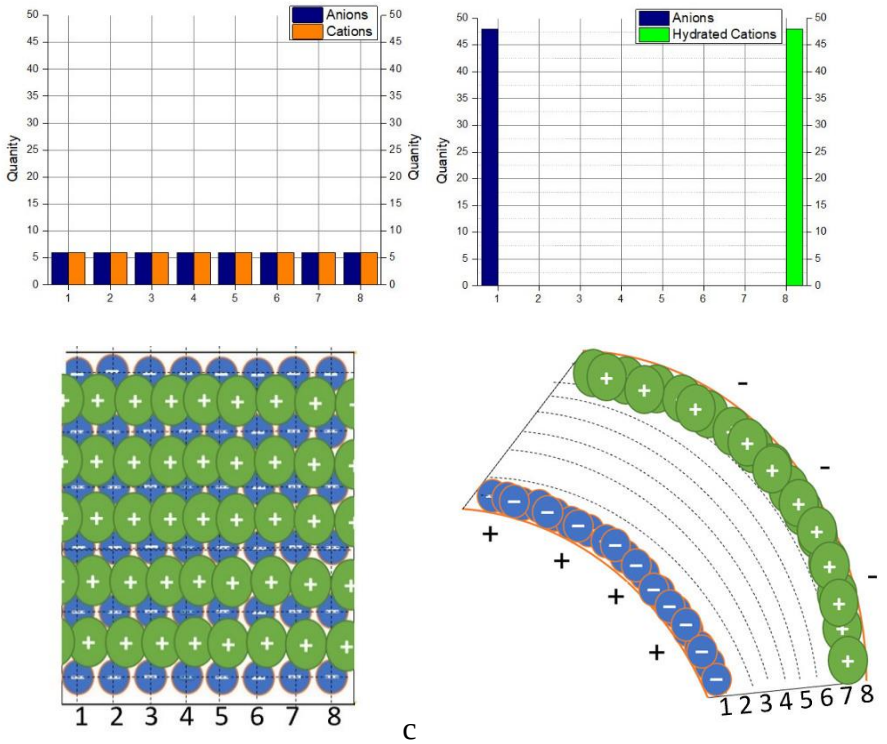

Figure 25: The process of ions accumulation of PVDF-LiP IPMC under electric filed.

What's more, there is interesting phenomenon named back relaxation only occur in PVDF-CoP IPMCs in high humidity level . Next chapter will

discuss the separate case. Therefore, the bending characteristics PVDF-CoP film is a topic which is worth studying under 3.5~4V DC.

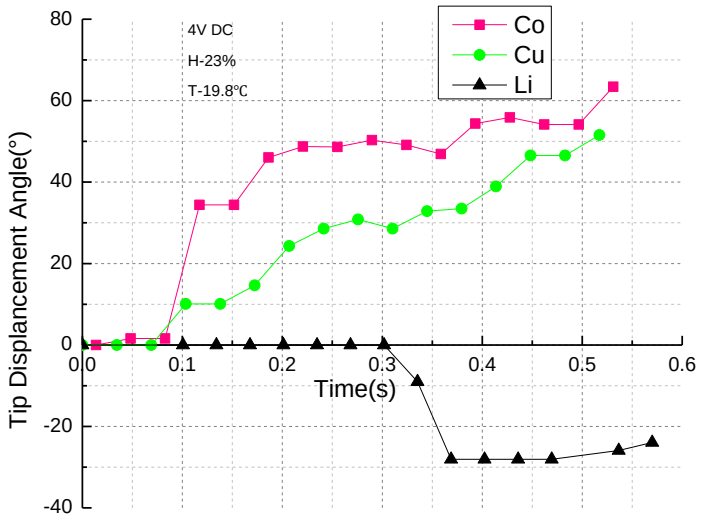

Figure 26: Tip displacement angle during the first 1 second of the actuation tests. The sample doped with Co2+ shows fastest response and maximum bending angle.

Figure 26 displays the response of deformation at the first 0.6s. PVDF-CoP IPMC shows quickest response (<0.1s) and largest cathode deformation (>60°). The response of PVDF doping with CuP is slow. While PVDF doping with li+ shows longest starting time and smallest anode bending. So PVDF-CoP IPMC has the potential to develop into an artificial insect wing under the AC voltage to manufacture microrobot.

3.5 Development of Accurately Fitting Method Based Electromechanical Bending Model

In this part, many models have been presented to fit the time-dependent result of *i*-EAP deformation under DC voltage. General speaking, black-box model only considers the experiment result while white-box model only takes

mechanism of bending into account. As for gray-box model, both mechanism and result must be considered.

Only according to bending data, it is followed an Arrhenius-like behavior using **Equation 3.1**.[2]

$$\mathrm{y} = \mathrm{A}e^{-\frac{B}{t}} \tag{3.1}$$

Rearranging

$$\ln y = -\mathrm{B}\left(\frac{1}{t}\right) + \ln A \tag{3.2}$$

Here, *B* is a constant about time while *y* can be any parameters about bending process such as strain, tip-displacement angle and radius of curvature. The relationship between stain and radius of curvature is shown in **Equation 3.3.**

$$\varepsilon = \frac{h}{2R} \tag{3.3}$$

Here, *h* is the sample thickness. *R* can be calculated if the sample is modeled as a sector. So, there is an equation is $\mathrm{s} = \mathrm{R}\theta$, where *s* is arc length. Chord length (*l*) is constant in whole bending process.

The boundary conditions are as follows.

$$\mathrm{t} = 0, \mathrm{y}(0) = 0 \tag{3.4}$$

$$\mathrm{t} = \mathrm{t}_{max}, \mathrm{y}(\mathrm{t}_{max}) = y_{max} \tag{3.5}$$

Table 5 displays Arrhenius-like Fitting parameters for PVDF-CoP with different DC voltages in low humility.

Table 5:Nonlinear and linear Arrhenius-like fitting parameters for PVDF IPMCs with different DC voltage

Sample	DC Voltage	Nonlinear fitting based on Equation 3.1			Linear fitting based on Equation 3.2		
		A (°)	B (s)	S_{max} (%)	A (°)	B (s)	S_{max} (%)
PVDF-15 wt.% Cop	3.5V	480.1	18.07	0.54	326.71	8.84	0.37
	4 V	549.9	11.85	0.62	450.24	9.30	0.51

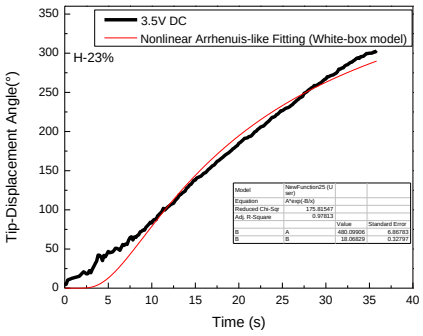

Figure 27: Nonlinear Arrhenius-like model of PVDF-based IPMCs with 15 wt.% CoP in 3.5V DC

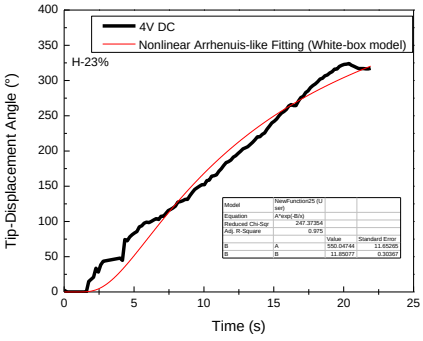

Figure 28:Nonlinear Arrhenius-like of PVDF-based IPMCs with 15 wt.% CoP under 4V DC

Nonmatter nonlinear or linear Arrhenius-like fitting, the black-box model cannot fit very well. The possible reason is the mechanism of bending is

ions accumulate at corresponding electrode rather than ions are activated and then move to different electrodes under DC voltage. It means that cation and anion redistribution and accumulation play a key role in the deformation of PVDF-based IPMCs.

Xiao and Bhattacharya developed a black-box model. The first-order differential equation is shown below. [3]

$$\frac{d\,k}{dt} = \frac{1}{\tau}(K_v V - k) \tag{3.6}$$

Rearranging

$$\mathrm{K(t)} = K_v V + C e^{-\frac{t}{\tau}} \tag{3.7}$$

Where K is curvature and K_v is the maximum curvature per unit extra voltage. V is extra voltage and τ is a constant only depend on time. C is a constant of integration.

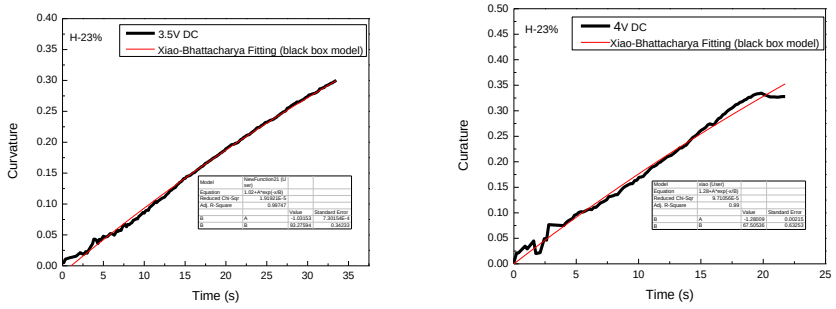

Figure 29:Nonlinear Xiao-Bhattacharya Fitting of PVDF-based IPMCs with 15 wt.% CoP under different DC fields

Presented in **Table 6** is the nonlinear Xiao-Bhattacharya Fitting parameters for PVDF-CoP with different DC voltage in low humility.

Table 6:The fitting parameters of Xiao-Bhattacharya's model of PVDF-based IPMCs with 15 wt.% CoP under different DC fields

Sample	Nonlinear fitting based on Equation 3.7			
PVDF+15wt% CoP	K_v	V	C	τ
	0.30	3.5	1.03	93.28
	0.33	4	1.28	67.51

According to **Figure 29**, it can be seen that Xiao-Bhattacharya's model does a better job to fitting the full time-dependence of the actuators. When fit analyzing, the factors of the redistribution and accumulation of cation and anion and curvature per unit extra voltage should be fully considered.

Based on comprehensive consideration of principles of physics and experiment data. Jain claimed that IPMC can be regarded as a uniform cantilever beam which undergo extra voltage. The IPMC system can be simplified to a RC circuits.

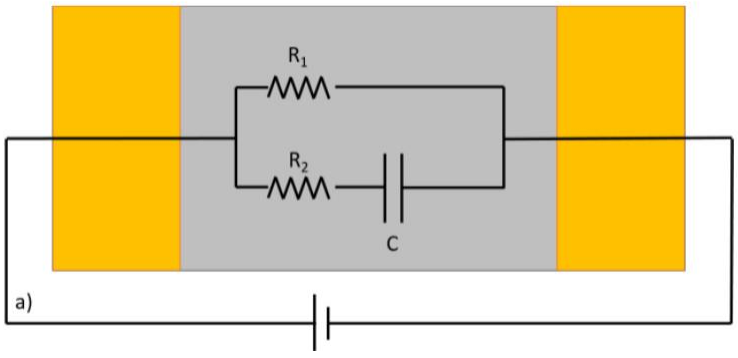

Figure 30: Jain's RC circuit model comparison for IPMC actuators

According to Kirchhoff's law, the system can be treated as a resistor in parallel with a second resistor and parallel plate capacitor (**Figure 30**). [4] If the individual resistor has a comparatively low resistance to the one in series with the capacitor, the charge distribution can be related both to the input voltage and to the induced bending moment generated in the film. Considering this model, the tip-displacement angle is a function of time. The equation is shown in **Equation 3.8**. [4]

$$\theta(t) = \frac{K}{b-a}e^{-at} + \frac{K}{a-b}e^{-bt} \tag{3.8}$$

Here, *k* relates to capacitance of polymer while both *a* and *b* are time constants.

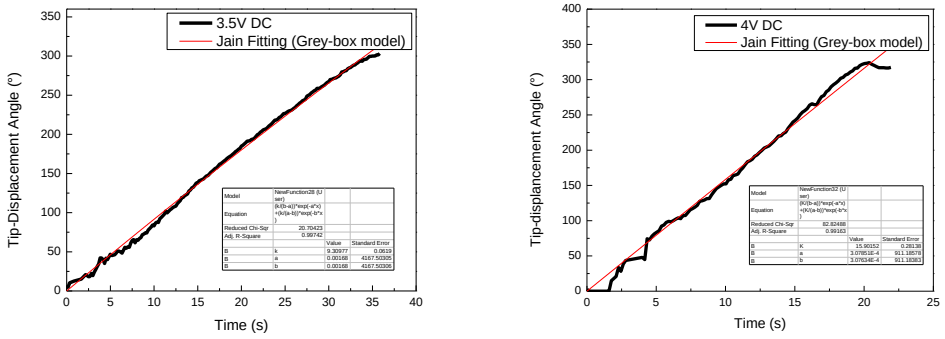

Figure 31: Nonlinear Jain Fitting of PVDF-based IPMCs with 15 wt.% CoP under different

Table 7:Nonlinear Jain fitting parameters for PVDF IPMCs with different DC voltages in low humility DC fields in low humility

Sample	Nonlinear fitting based on Eq.6			
PVDF +15wt% CoP	K	V	a	b
	9.31	3.5	$1.68*10^{-3}$	$1.68*10^{-3}$
	15.90	4	$3.07*10^{-4}$	$3.08*10^{-4}$

As has been clearly illustrated in this section, the Jain's gray-box model shows best fitting model and it can be also generalized to other polymer base IPMC which bending mechanism is accumulation of ions.

3.6 Variable-Humidity Testing of PVDF-CoP IPMCs

Interestingly, it is found that different bending behaviors of PVDF-CoP IPMC in different humidity levels. In lab, the range of humidity is 20~40%. So, three different relative humidity are generated by saturated sodium chloride solution and then pump to chamber. At the same time, temperature is constant about 20℃.Presented in **Figure 32** is the different bending behaviors.

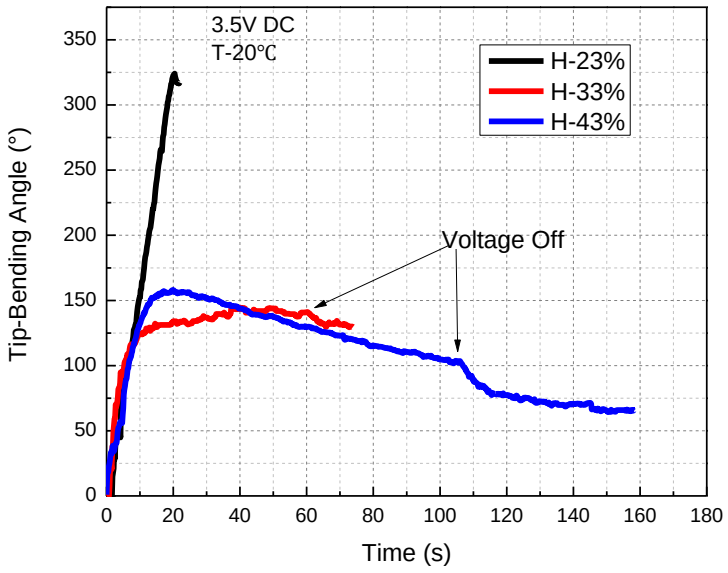

Figure 32：Different bending behaviors of PVDF-CoP IPMC in different humidity levels

Under low humidity condition, samples show maximum bending (>300°) after film be electrified. The bending angle is sharply decreased when the relative humidity up to 33%. 43% relative humidity causes cathode bending followed by a slow back relaxation deformation when voltage still applied. Back relaxation deformation is very common in other commercial IPMCs. Variable humidity has influence on bending angle rather than bending rate. 3.5V DC is applied to PVDF-base film doping with 15 wt.% CoP with a

thickness about 20 μm result in a new area of *i*-EAP research filed. Back relaxation will be followed by a discussion in **Chapter 4**.

Chapter 3 references

[1] Nightingale Jr E R. Phenomenological theory of ion solvation. Effective radii of hydrated ions[J]. The Journal of Physical Chemistry, 1959, 63(9): 1381-1387.

[2] Bass P. A Study on the Electromechanical/Dielectric Response of Poly (ethylene oxide)-Nanocrystalline-Cellulose Composites and Polyvinylidene Fluoride Electroactive Polymers[D].2016.

[3] Xiao, Y. and K. Bhattacharya. Modeling electromechanical properties of ionic polymers. in SPIE's 8th Annual International Symposium on Smart Structures and Materials. 2001.

[4] Jain, P., et al., Two IPMC fingers based micro gripper for handling. International Journal of Advanced Robotic Systems, 2011. 8(1): p. 1-9

Chapter 4 Bending Process and Back Relaxation of PVDF-CoP IMPC

4.0 Overview

For PVDF-Cop IPMC, the cathode deformation with back relaxation can be observed under 3.5V and 4V in 43% relative humility (**Figure 34**). Plots show typical positive relaxation. Films approach the maximin angle (about 160°) in a short time (<20s) and then relaxation occurred in a relative long time (more than 60s) under extra electric filed. When voltage off, the relaxation continued until get a new equilibrium position. To contrast with the actuation data which got in low humility (23%), there is no back relaxation and maximum bending angle is far larger than that in high humility. Therefore, the back relaxation is strongly sensitive with the air relative humidity.

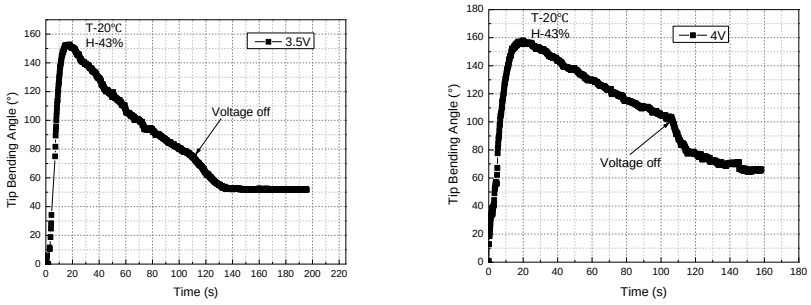

Figure 33: Positive back relaxation of PVDF-CoP IPMC under different voltages

Table 8:The actuation data of different stages under different voltages.

Sample	Voltage	Cathode deformation		Back relaxation		New equilibrium position	
		Angle (°)	Time(s)	Angle (°)	Time(s)	Angle (°)	Time(s)
PVDF-15 wt.% CoP	3.5 V DC	157	18	78	110	57	138
	4 V DC	158	22	100	106	63	143

For my sample, both cation and anion are move freely in polymer matrix. The mechanism of bending is ions accumulated at corresponding

electrode rather than water molecules redistribution. PVDF films doped with 15 wt.% CoP and CuP show significant cathode deformation following by positive back relaxation when humidity up to 43%. Positive back relaxation disappear in 33% relative humidity (RH) and maximum cathode deformation occurs in 23% RH. It is proved that the enplanement which hydrated cations go back to cathode side is incorrect. Because PVDF-CoP IPMC shows cathode deformation. If water molecules redistribution leads to osmotic pressure between cathode side and anode side, hydrated cations back will cause further cathode deformation rather than back relaxation.

4.1 The Mechanism of Back Relaxation

For PVDF doped with Li^+, samples still show large anode deformation without back relaxation in humidity from 23~43%. For commerce IPMCs, electrostatic stress and osmotic pressure may not be the real reason that films show back relaxation. Before test, Nafion-base IPMC was swamped in DI water. In actuator test process, water consent will decrease with time goes by. As the result, hydrated cations will loss water molecule continuously with water content decrease. It means that diameter of hydrated cation will decrease. After loss water molecule process, the diameter of hydrated cation smaller than that of anion, IPMCs will show negative back relaxation.

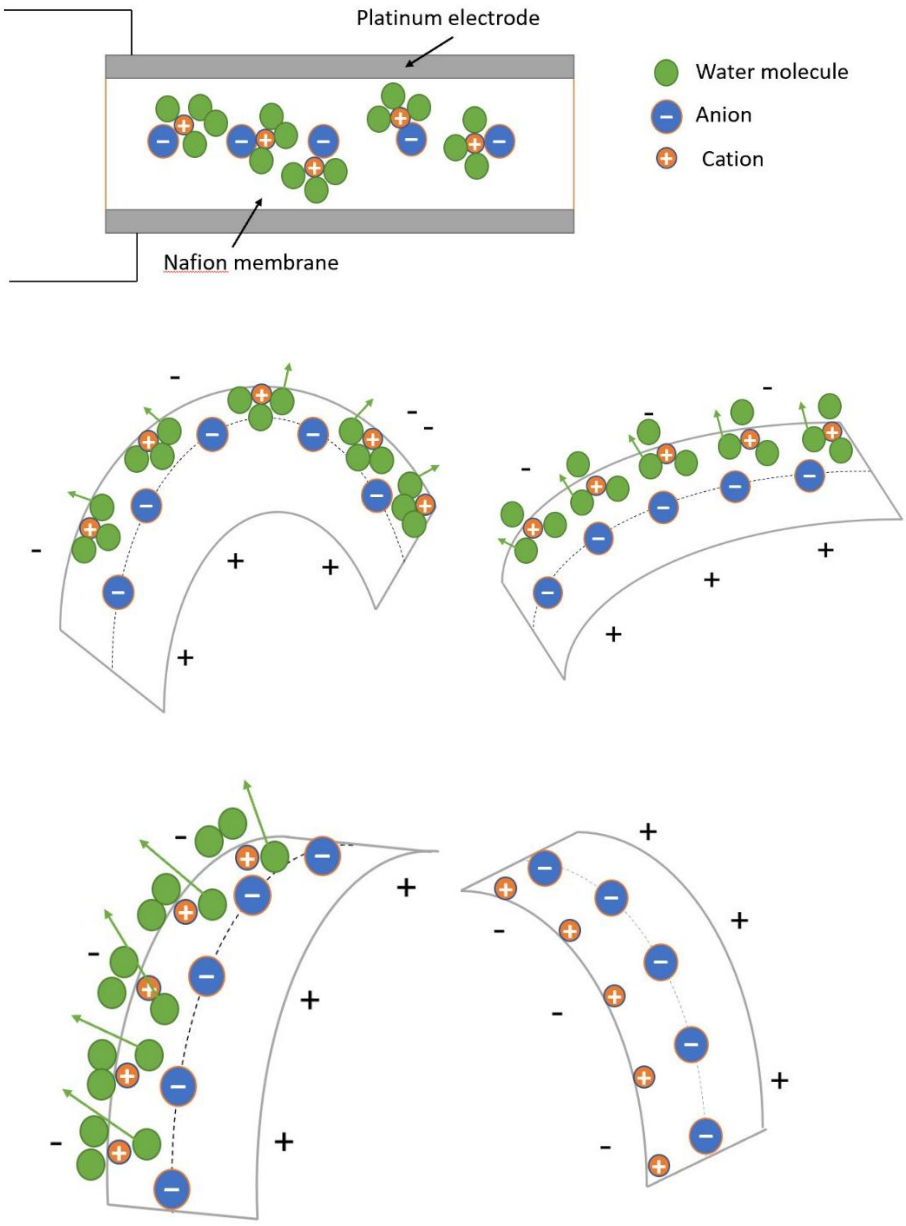

Figure 34: The schematic diagram of back relaxation

According to **Figure 34**, it is proved that water content has influence on back relaxation. If initial quantity of free water molecule is high enough, negative back relaxation will occur. Relaxation deformation will decrease with humidity until disappear when humidity low enough. Cathode deformation increase in high humidity level, and then decrease later at the same time. The

size difference between hydrated cation and anion is bigger than before when humidity decrease. When humidity continued to decrease, the hydrated cation becomes more and more scarce in IPMC. This has caused cathode deformation decrease until disappear when humidity low enough. So, there is peak of cathode deformation and back relaxation decreased continuously until disappear. For PVDF doped with 15 wt.% Cop IPMC, positive back relaxation disappear in 33% relative humidity (RH) and maximum cathode deformation occurs in 23% RH.

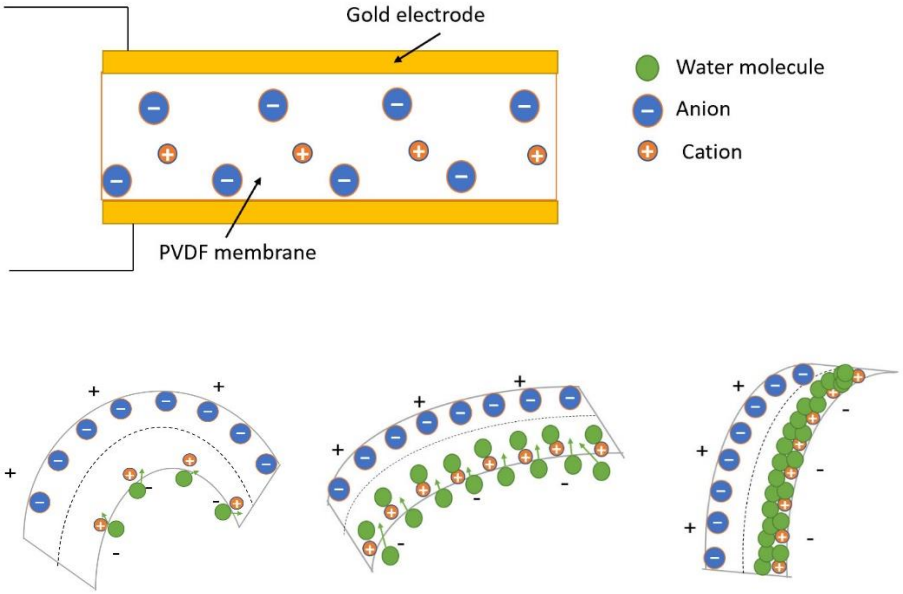

Figure 35：The mechanism of back relaxation of PVDF-CoP IPMC

Unlike other commerce IPMCs, PVDF-CoP IPMC shows large cathode deformation with positive back relaxation. There is an explanation that hydrated cations play a key role in back relaxation. After cations move and accumulate in cathode side under electric filed, ionic hydration occur. It means that water molecules are attract by cations to move into polymer base form air in high humidity. More and more water molecules are combined with cations lead to

increase the size of hydrated cations continuously. As the results, the size difference between hydrated cations and anions is becoming smaller and smaller. So, sample will relax a little bit after maximin bending angle. Additionally, IPMC will get a new equilibrium position rather than initial position. What's more, after multiple bending test in same sample, back relaxation will disappear. Maximin bending angle become smaller and bending speed is slower than that of first time at the same time. It is proved that the ionic size difference is becoming smaller and smaller with increase conduction time. The extra electric filed may accelerated ionic hydration reaction. It is the reason why PVDF doped with LiP show anode deformation without back relaxation in high humidity. (**Figure 35**)

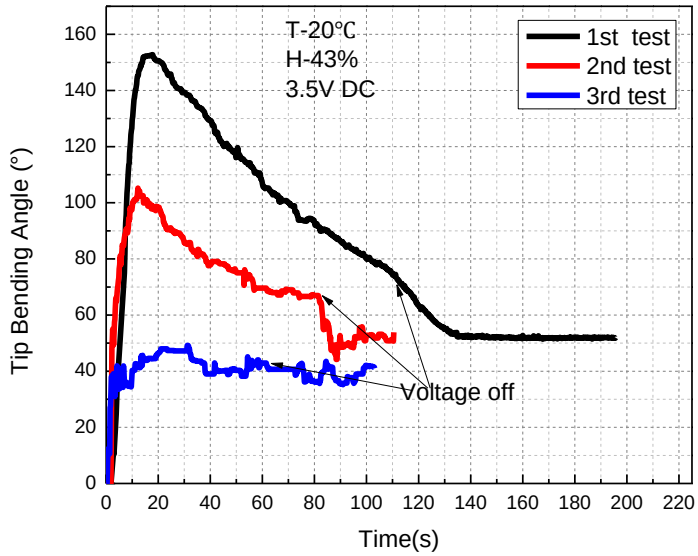

Figure 36: Positive back relaxation of same sample of different time test under 3.5V DC

The **Figure 36** illustrated that both maximum bending angle and final equilibrium position are decrease with increase test time in high humidity level. In the first test, sample obviously cathode deformation following by positive back relaxation. sample recover to an equilibrium position (50°). But the maximum bending angle is smaller than before in second test. In third test, sample shows a smallest bending without back relaxation. For fourth test, sample stand still at final equilibrium position. Cations accumulate in cathode side usually accompanies with ionic hydration reaction. Extra electric filed may promote the cations combined with water molecule. So, with test time increase, more and more water molecules are attracted into polymer from air. As the result, the diameter of hydrated cations is larger than that of bare cations. It means that the size different between hydrated cations and anions becomes smaller. From point of macroscopic view, back relaxation reduces gradually until disappear totally. At the same time, maximum bending angle will decrease.

It must be emphasized that back relaxation is harmful to emerging application. Back relaxation reduces the maximum of bending angle and makes response time longer. One challenge in IPMC actuators is how to mitigate the back relaxation. The article considers that, besides use Flemion to replace Nafion and choice metal which has high surface resistance as electrode, decrease water content in polymer base or test IPMC in low humidity level.

Chapter 5 Conclusion, Future work and Acknowledgements

5.1 Conclusions

A novel IPMC actuator based on PVDF was successfully developed. Glass transition temperature (Tg) was far lower than room temperature. Samples showed larger deformation because polymer in the rubbery state. In this state the mobility of polymer chains is high. Additionally, there was no branched chain for PVDF. Ions can move freely in polymer matrix. PVDF films doping with different ions were prepared by casting from solvent DMF. Gold was deposited on the two side of thin film as electrode. A new test system was established to monitoring whole bending and relaxation process. The thin strip of an PVDF-Base IPMC membrane was clamped between two copper clips to form a cantilever. Sample deformed into a circle followed by a slow back relaxation under a constant voltage. When voltage off, sample backed towards to a new equilibrium position, which is different from its initial position. PVDF film doping with 15 wt.% CoP is the first one of electroactive polymers which show large cathode deformation (>300°). 3.5V DC is lowest drive voltage and best electromechanical behavior is shown under 4V DC. If humidity very high (>43%), maximum bending angle was decrease and showed obviously positive back relaxation. It is widely accepted that the size difference between cations and anions generated strain after ions accumulated in corresponding electrode under electric filed. For back relaxation, we have reason to believe that hydration reaction of cations could largen the diameter of

hydrated cations. It leads to decrease the size difference between hydrated cations and anions. So, samples showed a little bite recovery and got a new position. The grey-box model could fit bending data very well because the model considered not only experiment data but also the mechanism of actuation.

5.2 Future Work

PVDF-base IPMCs has great potential for industrial application. A remarkable contribution of IPMC would be to see an artificial limb lift or grasp something using this technology in the future. Develop different types of IPMC has received significant interest for further master's and PhD's research. Even within couple chapters discuss, there are still many mysteries. So, the following research will focus on some areas: 1) For PVDF, to find other nontoxic solvent to replace DMF;2) To test more samples under AC voltage to encapsulate what will happen;3) Design an experiment to see how does the ionic hydration has influence on back relaxation; 4) After PVDF membrane cast form solution, samples should do annealing treatment and quench process to get different crystallinity film to see crystal region will block ionic motion or not;5) Using a load sensor to detect how many load can generate by IPMC; 6)Using MATLAB software or Python to editor a program which can monitor whole bending and back relaxation process in real-time;7) After hydration reaction occur, try to find a way to change hydration equilibrium. It means that water molecule should escape form hydrated cations after each bending and back relaxation. it

can help actuator to prolong lifetime of IPMC. It must be emphasized that PVDF-base IPMCs still have a long way to go.

5.3 Acknowledgements

I would like to present my great appreciation to my wife, Simin Wang, for them always stand by me. I would also want to thank my professor Dr. Zhongyang Cheng. He always pushing me and solving my puzzle. Without they support, this thesis would not be finished. Thank you for your ideas, Dr. Pengyu Chen and Dr. Edward Davis, as committee members. In the end, I am wholeheartedly grateful to other smart guys in my research group, namely, Ethan Hofer, Dr. Patrick Bass, Dr. Xu Lu, Dr. Yang Tong, Jiachen Liu, Liangxi Li and Steve Moore.